THE UNIVERSITY OF
NEW SOUTH WALES

SCHOOL OF ELECTRICAL ENGINEERING AND
TELECOMMUNICATIONS

Energy-Efficient Beamforming for Active IRS-aided JP-COMP Downlink Cell-edge Multiuser MISO Cellular Networks

By

Rui Yang

Thesis submitted as a requirement for the degree of

Master of Engineering Science (Telecommunications)

Submitted: Aug. 27, 2022

Abstract

This paper investigates an energy-efficient beamforming design for active intelligent reflecting surface (IRS)-aided joint processing coordinated multipoint (JP-CoMP) downlink cell-edge multiuser multiple input single output (MISO) cellular communication system. Generally, users in cell-edge would encounter additional inter-cell interference and an increase of path loss. IRS can be deployed to in wireless communication system to establish a controllable virtual channel that can improve the receiver quality. Besides, JP-CoMP allows multiple base stations (BSs) to share and transmit the transmission data to users, which can mitigate the inter-cell interference. We aim to maximize the energy efficiency of downlink cell-edge multiuser with the assistance of IRS and JP-CoMP by jointly optimize the beamforming vector of BSs and amplitude and phase shift matrix of IRS. The problem formulation also considers the quality of service (QoS) requirement for CUs, limitation of transmission power for each BSs and IRS, and limitation of communication backhaul capacity among BSs. In order to solve the non-convex problem, the proposed algorithm applies an iterative alternating optimization with successive convex approximation (SCA), semidefinite relaxation (SDR) and Dinkelbach method to resolve the sub-optimal solution that satisfies Karush-Kuhn-Tucker (KKT) condition. Simulation results demonstrate that by applying active IRS and JP-CoMP, we are able to achieve a high energy efficiency. In addition, it also illustrates that increase the number of IRS element and BS antennas could have a direct increase of energy efficiency.

Acknowledgements

Foremost, I would like to express my appreciate to my supervisor Derrick Wing Kwan Ng who made great contribution during my study of the project. He guided me not only in research field, but also in life. He encouraged me to think critically and teach me the key points of doing the research. Without his guidance, I wouldn’t be able to solve the problem in an efficient way. Due to his help, I developed a better understanding of the communication field. Also, I would like to thank all people that related to the progress this project.

Title: Energy-Efficient Beamforming for Active IRS-aided JP-COMP Downlink Cell-edge Multiuser MISO Cellular Networks

Topic number:

Student Name: Rui Yang **Student ID: z5337364**

A. **Problem statement**

The cell-edge cellular users usually encounter the worst communication quality due
to the inter-cell interference from different base stations. They also have a large
path loss as they are far from the cell. IRS can provide a better channel condition by
building an extra virtual channel through beamforming. There was many research
that used IRS as passive beamforming surface. There is an active IRS that focus on
both beamforming and amplification of signals but rarely researched. There are very
small number of maximizing the energy efficiency of cell-edge user with the help of
and JP-CoMP technology. It will be helpful for development of cell-edge
communication.

B. **Objective**

We aim to maximize the energy efficiency of downlink cell-edge multiuser
with the assistance of IRS and JP-CoMP by jointly optimize the beamforming
vector of BSs and amplitude and phase shift matrix of IRS.

C. **My solution**

Using iterative alternating optimization to solve non-convex problem
Using SCA to reduce complexity and transform the problem to convex
Using SDR to remove the non-convex rank constraint
Using Dinkelbach method to solve fractional programming

D. **Contributions** (at most one per line, most important first)

Defining the research topic
Determine the problem formulation
Develop the problem solution and algorithm
Work on the simulation of the algorithm
Analysis of simulation results

E. **Suggestions for future work**

Using multiple IRS for beamforming
Develop the problem with imperfect CSI
Try to extend the topic to MIMO system

While I may have benefited from discussion with other people, I certify that this report

is entirely my own work, except where appropriately documented acknowledgements are included.

Signature: Rui Yang Date: 02 / 08 / 2022

Pointers

7	Problem Statement
19	Objective

Theory

14	IRS structure
17	Independent diffusive scatterer-based model for IRS
20	The signal reflected and amplified by the active IRS
25	SDR theorem

Method of solution

23	Applying auxiliary optimization variables
25	SDR method
25	SCA method
26	Dinkelbach method

Contributions

32-33	Simulation results for energy efficiency and discussion
33-34	The effectiveness simulation for the algorithm
23,25,28	Problem transformation with auxiliary variables
27-32	Algorithm design

My work

19	System block diagrams/algorithms/equations solved
20	Description of assessment criteria used
19-21	Description of procedure (e.g. for experiments)

Results

33-34	Succinct presentation of results
32-34	Analysis
34	Significance of results

Conclusion

35-36	Statement of whether the outcomes met the objectives
36	Suggestions for future research

Literature:

26	Method of SCA
26	Reference to SDA
27	Material about Dinkelbach method
18	Model of IRS channel
12	Active IRS description

Contents

1 Introduction

With the development and deployment of fifth-generation (5G) structure in many countries, increased smartphone users are able to experience the benefits of 5G technologies. 5G is made up of many beneficial technologies of 5G include massive multi-input multi-output (MIMO), millimeter wave (mmWave) and so on. Massive MIMO is using large number of transmitter and receiver antennas to focus the energy to provide higher data rate and spectral efficiency. In terms of the mmWave communications, 5G focuses on using a specified range of short wavelength in millimeters to transmit wireless data, which is equivalent to a specified frequency range from 24GHz to 100GHz [1]. Higher frequency band can provide a wider bandwidth which can increase the communication capacity and data rate. In order to describe the performance of wireless communication system like 5G, there are many key performance indicators (KPIs) been proposed, which is shown in figure 1 [2]. In terms of the advantages of 5G, for example, it can provide a peak data rate of 20Gbps and experienced data rate of 0.1Gbps. 5G can achieve a peak energy efficiency of 30b/s/Hz. Currently, the infrastructure of 5G is still in progress and its performance will keep increasing. However, the step of scientific revaluation will not stop. The research and plans for sixth-generation (6G) have been conducted and designed to satisfy future requirements and applications.

Key Performance Indicator	5G	6G
System Capacity		
Peak Data Rate (Gbps)	20	1000
Experienced Data Rate (Gbps)	0.1	1
Peak Spectral Efficiency (b/s/Hz)	30	60
Experienced Spectral Efficiency (b/s/Hz)	0.3	3
Maximum Channel Bandwidth (GHz)	1	100
Area Traffic Capacity ($\mathrm{Mbps/m^2}$)	10	1000
Connection Density ($\mathrm{devices/km^2}$)	10^6	10^7
System Latency		
End-to-end Latency (ms)	1	0.1
Delay Jitter (ms)	NA	10^{-3}
System Management		
Energy Efficiency (Tb/J)	NA	1
Reliability (Packet Error Rate)	10^{-5}	10^{-9}
Mobility (km/h)	500	1000

Figure 1. The evolution from 5G to 6G wireless systems [2]

6G is envisaged to be a terrestrial wireless network that contains ubiquitous intelligence, reliability, scalability and security [1]. There are many new services and applications related to 6G, which includes immersive multi-sensory extended reality (XR), wireless power transfer (WPT), wireless multiple unmanned aerial vehicle (UAV) coordination, wireless brain-computer interactions and so on [3-6]. These new applications significantly improve the production efficiency for individuals and enterprises and experience of daily life. In order to fulfill the requirements of new applications, the brand-new KPIs for 6G is also illustrated in figure 1. In comparison with 5G, 6G wireless systems have a great improvement in many factors. For example, the peak data rate is 1000Gbps which increases five hundred times than 5G. Experienced data rate grows to 1 Gbps which is ten times more than 5G systems. Some of the not available KPIs are also measurable in 6G, which include delay jitter and energy

efficiency. Besides, other important KPIs such as experienced spectral efficiency, area traffic capacity, density, end-to-end latency and reliability will also be improved in 6G.

In order to fulfill this big vision, there are many solutions that are proposed for 6G. Some of the major technologies are, for example, networks that utilize terahertz frequency band which has plentiful spectral resource, large scale automation networks, cell-free massive MIMO communications and intelligent communication environments and so on [7]. Intelligent communication environment in 6G refers to technologies that can manage the wireless channel environment in a flexible way during transmission and reception. This report will focus on one intelligent communication environment, known as intelligent reflecting surface (IRS), and energy efficiency in wireless systems.

In wireless communication, cellular network is known as a radio network that distributes over a land area and signals are transmitted by base stations. It plays an important role in daily data transmission for smartphone users [8]. Currently, with the increasing number of communication devices such as smartphones in use, the total network capacity demands for cellular users are increasing. During the development of wireless communication, many contributions have been made in order to improve the quality of service and spectrum efficiency. For the upcoming sixth-generation (6G), many advanced communication technologies have been enhanced to meet the latest standard of data rate and capacity requirement. The technologies include ultra-density networks (UDNs), massive MIMO and mmWave communications [9-14]. However, to deploy these technologies in real world, designers need to withstand the large amount of power consumption and expensive hardware cost. In terms of the ultra-density networks, multiple base stations (BSs) are required in the region to support the large number of users. Large amount of power is required for the high-dense base stations transmitting power. Besides, mmWave communication, especially when it combines with MIMO technology to further increase the capacity, needs to feed the expensive RF-chains, and

afford a high complexity hardware cost [15][16]. As a result, applying these advance technologies would increase the users' cost when experience the fast speed and high signal quality.

In order to mitigate the high power consumption problem, 6G is considering an idea of green evaluation that focuses on the energy efficiency oriented design [17]. Recently, Intelligent reflecting surface has been proposed as an effective way to reduce the power consumption and provide energy-efficient solution for cellular users. As a promising new technology, IRS can manage to control the channel propagation environment by adjusting the phase of the wave in wireless communication. IRS is a programmable planner surface, which consists of a large amount of low-cost reflect elements. Each element is a square-shaped metallic patch unit, which can be designed using a printed dipole circuit or a phase shifter [18]. With the help of a controller chip, IRS can adjust the amplitude and phase of the impinging wave by configuring its elements to different states [19]. As it affects the propagation signals by passive reflection, IRS requires relatively low power, in comparison with transmitter RF-chains. Only the small dipole circuits on the elements and the IRS controller require power to operate. In terms of the advantages of IRS, by controlling the phase matrix of the reflective path, it can constructively increase the power gain at the receiver side along with the direct path [19]. In addition, if there is no direct path between the transmitter and receiver, IRS can help build a virtual line of sight by adjusting the signal direction, which can significantly improve the signal power gain [20]. In practice, IRS can be easily deployed or removed, and set to the cell-edge or shadowing area of BSs to enlarge the coverage area [21].

Generally, it is considered that in conventional IRS, the amplitude of the impinging wave does not get amplified. However, research on IRS indicate that there is an active-IRS design that can amplify both the amplitude and the phase of the propagation wave simultaneously, without significantly modify the

structure of IRS [22]. In comparison with traditional IRS, the active-IRS has an additional power source, and is able to boost the signal which experienced double pass loss effect [23]. The difference between active-IRS and full-duplex amplify-and-forward (FD-AF) relay is that the relay would introduce a delay during the amplification, meanwhile, active-IRS can amplify and reflect the signal at the same time without requiring extra delay [22]. By applying active-IRS aided cellular networks, the transmitted power at BS can be reduced, while at active-IRS the signal is amplified. Resource allocation algorithm can be performed to pursue the energy efficiency of the whole system [22].

Another objective for 6G is to provide a high data rate and quality at anywhere and anytime. In traditional cellular networks, the frequency passband can be reused at different BSs area separated by a reasonable distance for the sake of improvement of spectral efficiency. However, because of this frequency reuse in cellular networks, users in cell-edge can suffer the interference from different base stations while the power loss of the received signal would be great as it travels a long distance from the BS. Due to these two effects, users at BS cell-edge would have low signal to interference and noise ratio (SINR). In order to achieve ubiquitous access and quality of service, downlink joint processing coordinated multipoint (JP-CoMP) technology has been proposed. In JP-CoMP downlink cellular network, the users' data can be shared in multiple BSs using a central processor unit. The central processor unit will assign each user's data transmission task to multiple BSs to jointly transmit. The selection of BSs is based on the quality of service from BSs to the user, which is acquired from the shared channel state information (CSI). Different to MIMO technology, JP-CoMP can make use of the spatial degree of freedom, because it uses inter-cell transmission from different BSs [24]. Ideally, if the backhaul capacity is assumed to be infinite, the user's data can be shared to all the BSs and hence effective joint beamforming can be performed at all the BSs at the same time [25]. However, JP-CoMP has its limitation that the backhaul capacity among

BSs and central processing unit is not infinite. Therefore, in JP-CoMP network, only limited capacity of data can be shared and jointly transmitted for each BS in practice because of the expensive implementation cost [26]. As multiple BSs transmit data to a user simultaneously, the signal inter-cell interference for those users in cell-edge can be mitigated by utilizing JP-CoMP. In addition, JP-CoMP can increase the spectral efficiency as it is similar to the concept of MIMO that multiple input antennas are in different geographical location. Although the achieved spectral efficiency is restricted by the limited backhaul capacity to some extent, it is still an effective way to improve the quality of service and spectral efficiency for cellular users (CUs) in cell-edge.

In order to save energy while provide a good performance, in recent years, energy efficiency of the cellular network tend to become more and more popular in research. Energy-efficient cellular network design can be environmentally friendly and stimulate the economic growth. It could meet the users' data rate requirements without wasting addition energy. In other words, it aims to maximize the transmitted information rate per unit of energy, in bits/joules.

In this paper, our design will consider and combine the key technologies and concept discussed above, which include active-IRS, JP-CoMP and energy efficiency. It will focus on energy efficient beamforming for active IRS-aided JP-CoMP downlink cell-edge multiuser multiple input single output (MISO) cellular networks. Users in cell-edge usually suffer great path loss and inter-cell interference in downlink transmission, and it has been a long term challenge in cellular networks. By applying active-IRS and JP-CoMP, our design will provide an energy-efficient strategy to resolve this problem and provide the users an adequate quality of service. Meanwhile, our design will focus on MISO communication that the receiver only has one antenna. By applying this condition, the complexity of the system can be reduced.

2 Background

2.1 Intelligent reflecting surface (IRS)

A metamaterial is known as a man-made material, which is made from assembles of extremely small artificial elements (metallic or plastic) of subwavelength size. Metamaterial has properties that cannot be found in naturally synthesized materials. According to its small size, it is able to influence on external electromagnetic (EM) wave. In comparison with natural material, metamaterial has unique EM properties, which include controlling its equivalent permeability and permittivity by adjusting the shape, size and inside structure of atoms in space [19]. During 2011 and 2012, the idea of metasurface was first proposed [27]. The metasurface can be regarded as a two-dimensional surface that consist of array of passive scattering elements. The magnitude and direction of the impinging EM wave between two different medias is following the Snell's law and Fresnel equations [28]. However, in metasurface, the situation is different that the arrangement of scattering elements could cause different boundary conditions, thus it can provide an extra phase change [29]. Different to the traditional three-dimensional EM elements, such as waveguide, to adjust the direction, amplitude and phase of EM wave, metasurface can achieve the same goal on its surface and the required thickness is less than the wavelength of EM waves. Therefore, it can reduce the cost of the material and easier to manufacture as it is two-dimensional.

In general, once the metasurface is manufactured, its EM properties will be fixed and serve a specific condition [29]. However, it is not flexible and cannot deal with situation that has other purpose or operates in different frequency. With the development of EM metamaterials, the concept of intelligent reflecting surface (IRS), also known as reconfigurable intelligent surface (RIS), was proposed, so that it is able to program and control the phase shift of the

impinging EM wave. The EM properties of IRS can be modified by performing external stimuli on the scattering elements [30]. In terms of the structure of IRS, it contains an array of passive scattering elements, tunable chips or PIN switches, a PCB substrate and embedded controller, which is shown in figure 2. Tunable chips or PIN switches can be used to provide external stimuli to the elements to reconfigure its EM properties. The embedded controller is to control the configuration of tunable chips or PIN switch to provide different phase shift which can satisfy different conditions. Due to its two-dimensional feature, IRS can be easily deployed or removed from the building or wall. In addition, IRS is considered to be a passive power resource as it only reflects the EM wave rather than uses antennas to transmit the signal.

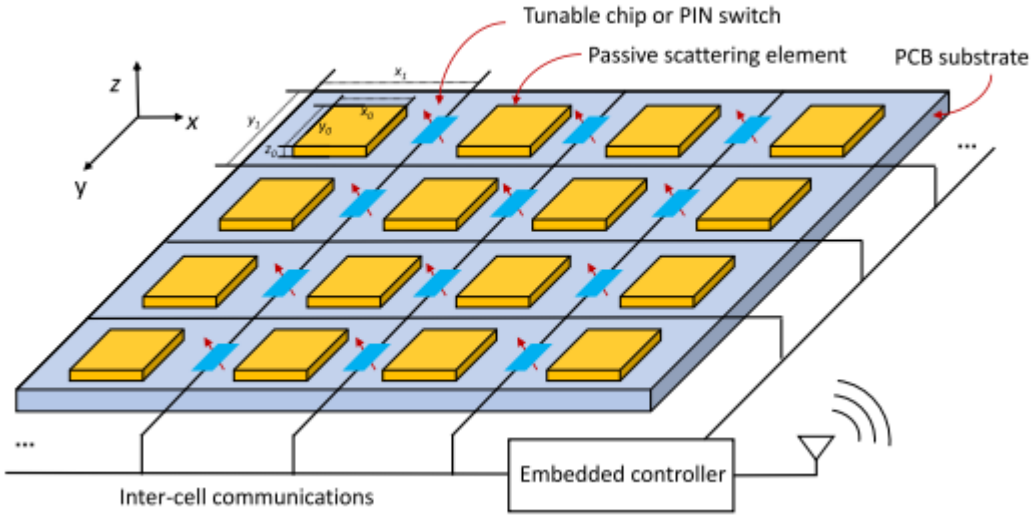

Figure 2. The structure of IRS [29]

As a promising wireless communication technology, IRS has many advantages and can be applied in many situations. Firstly, IRS can be easily deployed in many places such as the windows on the building, walls, cars and even on human bodies [21]. Secondly, IRS is environmentally friendly, which only consumes a small amount of power when operating as a passive beamforming device. In terms of applications, it can be used in signal enhancement for systems such as non-orthogonal multiple access (NOMA), massive device-to-device (D2D) communications and wireless power transfer. In addition, it can

also be used in holographic imaging due to its high ability to adjust EM waves. There are many scenarios of IRS-aided wireless communications, which is shown in figure 3. For outdoor environment, it can be deployed on the wall to provide a virtual line of sight for cellular users, when the direct path from the base stations is blocked and users are experiencing bad quality of signals. In other words, deployment of IRS can increase the power gain at users and the coverage of cellular networks. If there is a direct path from BS and users, the reflect path from IRS can be constructively combined with the direct path to further increase the power gain at the receiver. On the other hand, IRS can control the environment to destructively combined with the signal at the unwanted users to cancel out the information for security reason. In terms of indoor environment, IRS can be set to the wall close to the window to provide a better signal quality to users inside the building. A joint beamforming of BS transmitter antenna and IRS passive reflection can be formed in order to optimize the spectrum efficiency or energy efficiency problem.

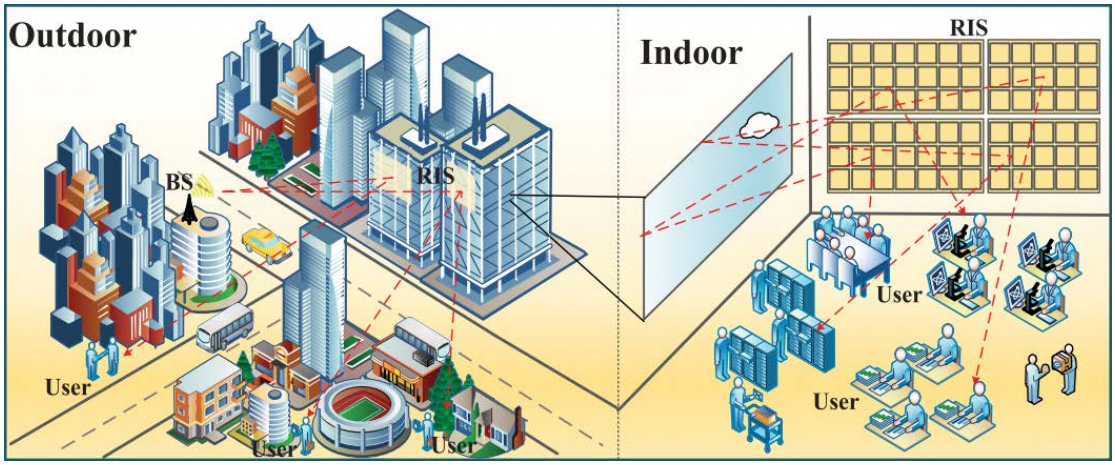

Figure 3. Outdoor and indoor applications of IRS-aided wireless communication [19]

Over the past few years, many innovative and useful optimization research towards IRS-aided wireless system have been conducted. In [31], a design of resource allocation for full-duplex cognitive radio systems is derived, which serves both half-duplex uplink and downlink users at the same time. In [32], a power-efficient resources allocation based on IRS-aided multiuser systems was

formulated and optimized using inner approximation (IA) algorithm. With regard to IRS-assisted simultaneous wireless information and power transfer (SWIPT) [33], an idea of seeking energy efficiency in a secure IRS-assisted SWIPT system using alternating optimization (AO) algorithm has been discussed [34]. Besides, [35] resolved the optimization problem in IRS-aided SWIPT, which considered the tradeoff between the maximization of data sum rate and the maximization of total harvested energy. A self-sustainable optimizing IRS design has been conducted by fully usage of IRS elements for both phase shift and energy harvesting purpose to compensate the IRS power consumption [36]. In terms of the advantages of IRS in UAV wireless communication, in [37], it maximized the energy efficiency in UAV system with secure constraints to fulfill the requirements of different users based on their preferred security levels. Other research related to IRS-aided UAV include the sensing and intelligence of 5G and beyond UAV overview [38], 3D-trajectory design for a solar-powered UAV communication [39] and a power-efficient UAV-NOMA communication system [40]. In terms of the security area, in [41], the author considered the application of IRS in secure wireless system. IRS is used to increase the robustness of wireless communication [42], green communication system [43], sum-rate maximization [44] and beamforming of NOMA-based IoT with SWIPT [45]. Another research related to NOMA is finding the performance gain of NOMA and orthogonal multiple access uplink communication system [46]. The resource allocation problem for joint optimization of the beamforming vector and artificial noise at BS and passive beamforming matrix at IRS was formulated and resolved. Research on Massive non-orthogonal multiple access with imperfect successive interference cancellation has been conducted [47]. In addition, double IRS-assisted system has been considered and designed for MIMO mmWave communications [48]. Moreover, in deep residual learning area, IRS is also used for channel estimation multi-user system [49] and research on edge learning for B5G network with semantic communication [50].

In terms of the IRS modeling in our design, independent diffusive scatterer-

based (IDS) model is selected due to its low complexity and relatively accurate description of IRS reflection. IDS is a widely used model in literature review of IRS-aided wireless communication. As shown in figure 4, it assumes that each scattering element in IRS can provide a separate phase shift for the impinging EM waves [51]. Therefore, the total IRS can be represented as a diagonal matrix $\boldsymbol{\Theta} = diag(\beta_1 e^{j\theta 1}, \cdots, \beta_M e^{j\theta M})$, which is known as phase shift matrix [52]. Inside the matrix, the diagonal values are the reflection factors, where β_m and $e^{j\theta m}$ stands for the amplitude and phase shift at IRS element m. In traditional IRS design, the amplitude β_m is usually set to one for simplicity. However, in our design β_m will not be one as an active-IRS will be utilized which can amplify the reflected signals.

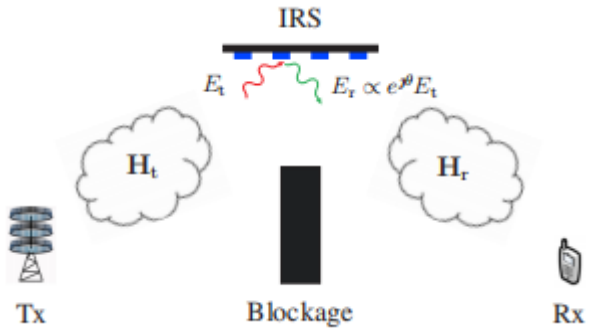

Figure 4. Independent diffusive scatterer-based model for IRS [52]

In order to further improve the performance of IRS, the idea of active IRS has been proposed, which can adjust both the phase and amplitude of EM wave simultaneously by adding an extra power supply in IRS [22]. In comparison with general IRS, active IRS can provide better quality of service for cellular users with a proper recourse allocation. Active IRS-aided wireless system could reduce the required power at BSs and compensate the signal loss at IRS side while the whole required power can be reduced. Therefore, with the assistance of active IRS, our design is able to provide a better energy efficient solution.

2.2 Joint processing coordinated multipoint

One of the key concepts of 6G is to provide ubiquitous access with high capacity. In current 4G and 5G communication, MIMO-orthogonal frequency division multiplexing (OFDM) is utilized in Long Term Evolution (LTE) to achieve better spectral efficiency. However, in terms of cellular users in cell-edge, they usually suffer a slow data rate and interference from other BSs. MIMO-OFDM can increase the spectral efficiency within one cell, but it cannot mitigate the interference from other cells [53]. In order to decrease the impact of multi-cell interference, coordinated multipoint (CoMP) transmission is proposed as a promising technology. CoMP is able to increase the cell-edge users' data rate and spectral efficiency by sharing and transmit the users' data among BSs. There are two types of CoMP transmission: joint processing coordinated multipoint (JP-CoMP) and coordinated beamforming coordinated multipoint (CB-CoMP) transmission. For JP-CoMP, the user's data is shared among multiple BSs and these BSs will transmit the same data information through inter-cell transmission at the same time. In other words, the data will be constructively received at user side and the inter-cell interference is reduced. In contrast, CB-CoMP is only using one BS to transmit the user's data while communicating to other BSs and modify the beamforming of other BSs to reduce the inter-cell interference. In our design, the JP-CoMP is applied as it can exploit the spatial degree-of-freedom from multiple BSs. In order to communicate and share the users' data, an extra central processing unit is required for JP-CoMP system. Since there is also a backhaul capacity between central processing unit and each BS, the limited backhaul capacity will be considered in this design, as it is not infinity and could lead to a cost.

3 System model and Problem Formulation

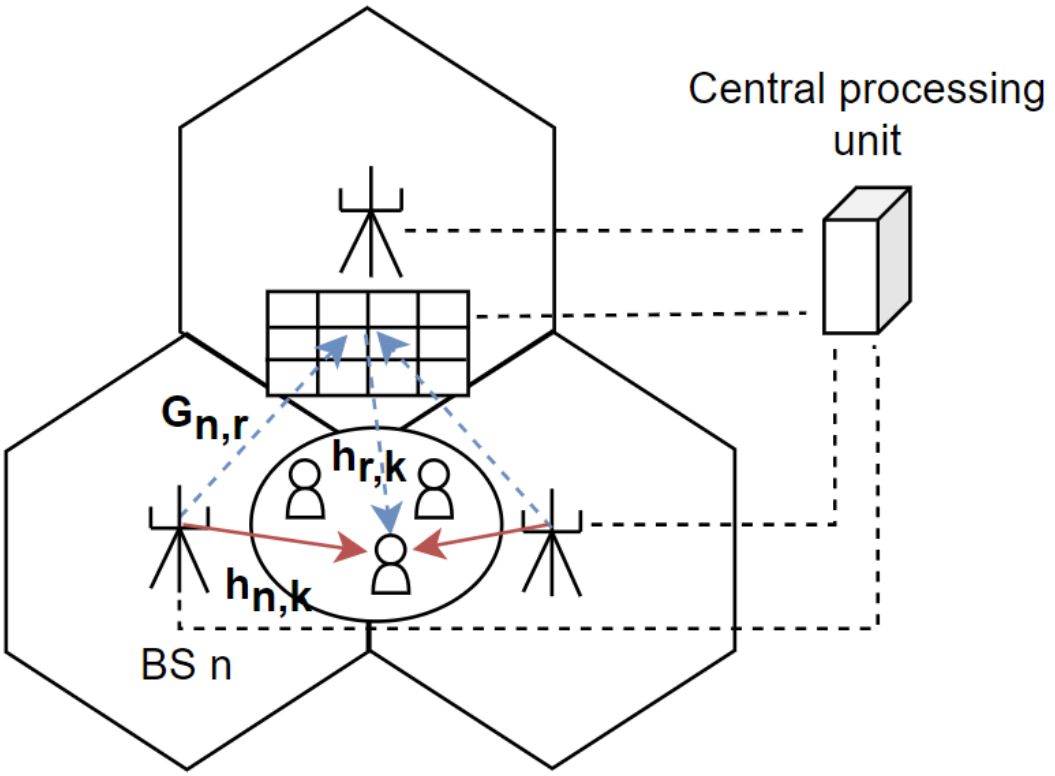

Figure 5. A system model of IRS-aided JP-CoMP multiuser MISO networks

Our design focuses on cell-edge active IRS-aided joint processing coordinated multipoint (JP-CoMP) downlink MISO cellular networks. We aim to maximize the network energy efficiency (EE) by jointly optimizing the transmit beamforming at BSs and the phase shift matrix at the IRS. We take into account the quality of service (QoS) for each cellular user, the total power transmits at the BSs, the limited backhaul capacity, and the maximum power allowance of the amplification power for active IRS.

In this system, as shown in figure 5, we assume that there are *N* BSs and *K* cellular users (CUs). Each base station is equipped with $N_t > 1$ transmit antennas and each user is equipped with one antenna. The IRS is equipped with *M* reflecting elements. All the BSs and IRS are connected to a central processing unit with a limited backhaul capacity. Denote the transmit

beamforming vector and binary transmitted signal as $\boldsymbol{w}_{n,k} \in \mathbb{C}^{N_T \times 1}$ and $s_k \sim CN(0,1)$. Let $\boldsymbol{G}_{n,r} \in \mathbb{C}^{N_T \times M}$, $\boldsymbol{h}_{n,k} \in \mathbb{C}^{N_T \times 1}$, $\boldsymbol{h}_{r,k} \in \mathbb{C}^{M \times 1}$ donate the complex equivalent baseband channels of BS n-to-IRS, BS n-to-user k, IRS-to-user k. The complex baseband transmitted signal $\boldsymbol{x}_n$ at the BS n is given by:

$$\boldsymbol{x}_n = \sum_{k \in K} a_{n,k} \boldsymbol{w}_{n,k} s_k \,, \tag{1}$$

where

$$a_{n,k} = \begin{cases} 1, if\ user\ k\ is\ linked\ with\ BS\ n, \\ 0, otherwise. \end{cases} \tag{2}$$

The signal reflected and amplified by the active IRS is given by:

$$\boldsymbol{y} = \underbrace{\boldsymbol{B\Theta}\left(\sum_{n=1}^{N} \boldsymbol{G}_{n,r} \boldsymbol{x}_n\right)}_{Amplified\ signal} + \underbrace{\boldsymbol{B\Theta d}}_{\substack{Dynamic \\ noise}} + \underbrace{\boldsymbol{e}}_{\substack{static \\ noise}} , \tag{3}$$

where we define $\boldsymbol{\Theta} = diag(e^{j\theta 1}, \cdots, e^{j\theta M})$ and $\boldsymbol{B} = diag(\beta_1, \beta_2, \ldots, \beta_M)$ as the phase shift and amplification factor matrix for IRS elements. $\boldsymbol{d} \in \mathbb{C}^{N_T \times 1}$ is modelled as additive white Gaussian noise (AWGN) with variance σ_d^2, i.e., $\boldsymbol{d} \sim CN(0_{N_T}, \sigma_d^2 I_{N_T})$, The static noise $\boldsymbol{e} \in \mathbb{C}^{N_T \times 1}$ is modelled as AWGN with variance σ_e^2, i.e., $\boldsymbol{e} \sim CN(0_{N_T}, \sigma_e^2 I_{N_T})$.

The received signal at user k:

$$\begin{aligned} y_k &= \sum_{n=1}^{N} \boldsymbol{h}_{n,k} x_n + \boldsymbol{h}_{r,k} \boldsymbol{B\Theta} \sum_{n=1}^{N} \boldsymbol{G}_{n,r} \boldsymbol{x}_n + \boldsymbol{h}_{r,k} \boldsymbol{B\Theta d} + n_k \\ &= \sum_{n=1}^{N} \left(\boldsymbol{h}_{n,k} + \boldsymbol{h}_{r,k} \boldsymbol{B\Theta G}_{n,r}\right) a_{n,k} \boldsymbol{w}_{n,k} s_k \\ &+ \sum_{n=1}^{N} \sum_{j \neq k}^{K} \left(\boldsymbol{h}_{n,k} + \boldsymbol{h}_{r,k} \boldsymbol{B\Theta G}_{n,r}\right) a_{n,j} \boldsymbol{w}_{n,j} s_j + \boldsymbol{h}_{r,k} \boldsymbol{B\Theta d} + n_{k.} \end{aligned} \tag{4}$$

For notation simplicity, we define $\bar{\boldsymbol{H}}_{n,k} = \boldsymbol{h}_{n,k} + \boldsymbol{h}_{r,k} \boldsymbol{B\Theta G}_{n,r}$,

$\bar{\boldsymbol{H}}_k = [\bar{\boldsymbol{H}}_{1,k}, \bar{\boldsymbol{H}}_{2,k}, \ldots, \bar{\boldsymbol{H}}_{n,k}]$, $\boldsymbol{A}_{n,k} = diag(a_{n,k}, \ldots, a_{n,k})$,

$\boldsymbol{A}_k = diag(\boldsymbol{A}_{1,k}, \ldots \boldsymbol{A}_{n,k})$ and $\overline{\boldsymbol{W}}_k = [\boldsymbol{w}_{1,k}^H, \boldsymbol{w}_{2,k}^H, \ldots, \boldsymbol{w}_{n,k}^H]^H$. The SINR for user k:

$$\gamma_k = \frac{|\overline{\boldsymbol{H}}_k^H \boldsymbol{A}_k \overline{\boldsymbol{W}}_k|^2}{\sum_{j\neq k}^{K} \left|\overline{\boldsymbol{H}}_j^H \boldsymbol{A}_j \overline{\boldsymbol{W}}_j\right|^2 + \sigma_d^2 \left\|\boldsymbol{H}_{r,k}^H \boldsymbol{B}\boldsymbol{\Theta}\right\|^2 + \sigma_{n_k}^2}. \quad (5)$$

The total sum information rate for the system is:

$$R = \sum_{k=1}^{K} \log(1+\gamma_k). \quad (6)$$

Total power P_{tot} that required for the system:

$$P_{tot} = \sum_{n=1}^{N}\sum_{k=1}^{K} a_{n,k}\left\|\boldsymbol{w}_{n,k}\right\|^2 + Pc + \sum_{k=1}^{K}\left(\left\|\sum_{n=1}^{N} \boldsymbol{B}\boldsymbol{\Theta}\boldsymbol{G}_{n,r} a_{n,k}\boldsymbol{w}_{n,k}\right\|^2\right) + \sigma_d^2\|\boldsymbol{B}\boldsymbol{\Theta}\|^2, \quad (7)$$

where *P*c refers to the required constant circuit power for one IRS phase shifter. On the other hand, the limited backhaul capacity for BS n:

$$\sum_{k=1}^{K} a_{n,k}\log(1+\gamma_k) \leq C_n, \forall n \quad (8)$$

where C_n denotes the constant limited backhaul capacity that BS n can afford. We assume $a_{n,k}$ is predefined by considering the CSI, which will be fixed during the optimization process. Our goal is to maximize EE:

$$\text{P1:} \quad Maximize_{\boldsymbol{w}_{n,k},\boldsymbol{\theta},\boldsymbol{B}} \frac{R}{P_{tot}} \quad (9)$$

$$\text{s.t} \quad \text{C1:} \sum_{k=1}^{K} a_{n,k}\left\|\boldsymbol{w}_{n,k}\right\|^2 \leq P_{max}, \forall n, \quad (9.1)$$

$$\text{C2:} \sum_{k=1}^{K} a_{n,k}\log(1+\gamma_k) \leq C_n, \forall n, \quad (9.2)$$

$$\text{C3:} \gamma_k \geq \gamma_{min}, \forall k, \quad (9.3)$$

$$\text{C4:} 0 \leq \theta_m \leq 2\pi, \forall m, \quad (9,4)$$

$$\text{C5:} \sum_{k=1}^{K}\left(\left\|\sum_{n=1}^{N} \boldsymbol{B}\boldsymbol{\Theta}\boldsymbol{G}_{n,r} a_{n,k}\boldsymbol{w}_{n,k}\right\|^2\right) + \sigma_d^2\|\boldsymbol{B}\boldsymbol{\Theta}\|^2 \leq P_A. \quad (9.5)$$

In the optimization problem, $\boldsymbol{w}_{n,k}, \boldsymbol{\theta}, \boldsymbol{B}$ are three optimization variables. In terms of constraint C1, $P_{max} > 0$ is a constant that represents the maximum allowance power at a base station. C2 is the backhaul capacity constraint, where $C_n > 0$ is a constant. C3 is the requirement of minimum quality of service for each cellular user, where $\gamma_{min} > 0$ stands for the minimum user received SINR. C4 is the phase shift constrain for IRS. C5 specifies the

maximum allowance power that the active IRS can amplified and constant $P_A > 0$.

For the problem formulars above, the objective function P1 is non-convex as γ_k and P_{tot} are non-convex, which means there can be multiple local optimums. Solving non-convex problem would take huge amount of time because all the local minimum values are required to be found in order to determine the global optimum solution. A possible solution might be finding a local optimum. In terms of the constrains, C1 and C4 are convex. On the other hand, for C2, C3 and C5, they are non-convex constrains, because γ_k is non-convex and optimization variables are coupled in these formulars. Therefore, the whole optimization problem P1 is non-convex. A possible way to solve non-convex problem is to find its suboptimum values, which requires lower complexity. Further problem solving process will be derived in thesis B.

4 Solution of the optimization problem

To start with, P1 is non-convex problem as it has 3 coupled optimization variables $\boldsymbol{w}_{n,k}, \boldsymbol{\theta}, \boldsymbol{B}$ multiplying to each other. Compared to spend large amount of time to work out the global optimal value, it is easier to find the local optimal value. The alternating optimization method will be applied to find out the local optimal value. It solves each of the variables separately while the other two variables are fixed. Then concurrently solve the other two in one iteration until the problem converges. Furthermore, in each subproblem, the success convex approximation (SCA), semidefinite relaxation (SDR) and Dinkelbach method are also utilized to facilitate our optimization. The overall design diagram is shown below in figure 6.

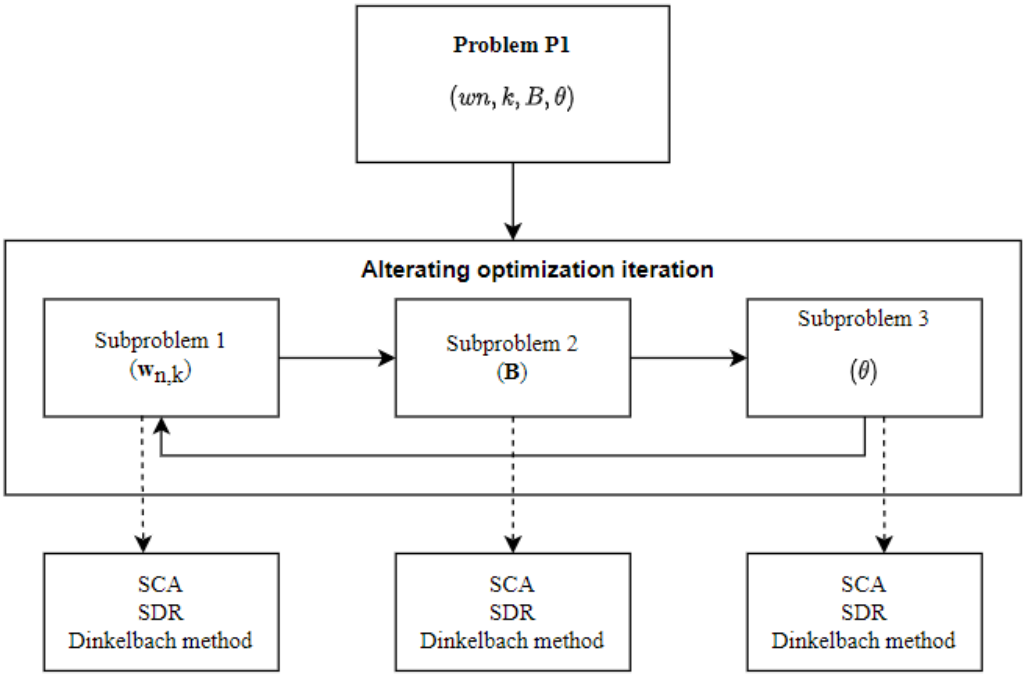

Figure 6. Overview diagram of the optimization design.

4.1 subproblem 1: beamforming optimization

Firstly, we consider solving the beamforming vector $\boldsymbol{w}_{n,k}$ subproblem while the $\boldsymbol{\theta}, \boldsymbol{B}$ are seen as fixed values. Before we work out the convergence, the SINR can be simplified in order to reduce the complexity. It becomes:

$$R = \sum_{k=1}^{K} \log(1+\gamma_k) = \sum_{k=1}^{K} \log\left(1 + \frac{|\overline{\boldsymbol{H}}_k^H \boldsymbol{A}_k \overline{\boldsymbol{W}}_k|^2}{\sum_{j\neq k}^{K} \left|\overline{\boldsymbol{H}}_j^H \boldsymbol{A}_j \overline{\boldsymbol{W}}_j\right|^2 + \sigma_d^2 \left\|\boldsymbol{H}_{r,k}^H \boldsymbol{B}\boldsymbol{\Theta}\right\|^2 + \sigma_{n_k}^2}\right)$$
$$= \sum_{k=1}^{K} \log\left(1 + \frac{\tau_k}{\beta_k}\right) = \sum_{k=1}^{K} \log(\beta_k + \tau_k) - \log(\beta_k), \qquad (10)$$

where τ_k and β_k are auxiliary optimization variables for simplicity. After we substitute τ_k and β_k into the subproblem, the subproblem (10) becomes:

$$Maximize_{\boldsymbol{w}_{n,k},\tau_k,\beta_k} \frac{\sum_{k=1}^{K} \left(\log\left(\beta_k + \tau_k\right) - \log\left(\beta_k\right)\right)}{\sum_{n=1}^{N}\sum_{k=1}^{K} a_{n,k}\left\|\boldsymbol{w}_{n,k}\right\|^2 + Pc + \sum_{k=1}^{K}\left(\left\|\sum_{n=1}^{N} \boldsymbol{B}\boldsymbol{\Theta}\boldsymbol{G}_{n,r} a_{n,k}\boldsymbol{w}_{n,k}\right\|^2\right) + \sigma_d^2\|\boldsymbol{B}\boldsymbol{\Theta}\|^2}$$

$$\text{s.t} \quad \text{C1}: \sum_{k=1}^{K} a_{n,k}\left\|\boldsymbol{w}_{n,k}\right\|^2 \leq P_{max}, \forall n, \qquad (11.1)$$

$$\text{C2}: \sum_{k=1}^{K} a_{n,k} \quad (\log(\beta_k + \tau_k) - \log(\beta_k)) \quad \leq C_n\,, \forall n, \tag{11.2}$$

$$\text{C3}: \log(\beta_k + \tau_k) - \log(\beta_k) \geq R_{k,min}, \forall k, \tag{11.3}$$

$$\text{C4}: \tau_k \leq |\overline{\boldsymbol{H}}_k^H \boldsymbol{A}_k \overline{\boldsymbol{W}}_k|^2 \tag{11.4}$$

$$\text{C5}: \beta_k \geq \sum_{j\neq k}^{K} \left|\overline{\boldsymbol{H}}_k^H \boldsymbol{A}_j \overline{\boldsymbol{W}}_j\right|^2 + \sigma_d^2 \left\|\boldsymbol{H}_{r,k}^H \boldsymbol{B}\boldsymbol{\Theta}\right\|^2 + \sigma_{n_k}^2 \tag{11.5}$$

$$\text{C6}: \sum_{k=1}^{K} \left(\left\| \sum_{n=1}^{N} \boldsymbol{B}\boldsymbol{\Theta}\boldsymbol{G}_{n,r} a_{n,k} \boldsymbol{w}_{n,k} \right\|^2 \right) + \sigma_d^2 \|\boldsymbol{B}\boldsymbol{\Theta}\|^2 \leq P_A. \tag{11.6}$$

Compared to the original problem, the formulated subproblem has three optimization variables $\boldsymbol{w}_{n,k}, \tau_k, \beta_k$. Constrain C4 in (9.4) is not included as it is not related to any of these three variables. Besides, two additional constrains C4 (10.4) and C5 (10.5) are added as we need to declare the relationship of the auxiliary optimization variables and their substitution. As our goal is to maximize the energy efficiency, τ_k cannot go over $|\overline{\boldsymbol{H}}_k^H \boldsymbol{A}_k \overline{\boldsymbol{W}}_k|^2$ and β_k cannot be less than $\sum_{j\neq k}^{K} \left|\overline{\boldsymbol{H}}_k^H \boldsymbol{A}_j \overline{\boldsymbol{W}}_j\right|^2 + \sigma_d^2 \left\|\boldsymbol{H}_{r,k}^H \boldsymbol{B}\boldsymbol{\Theta}\right\|^2 + \sigma_{n_k}^2$. Therefore, we can make sure that we wouldn't go over the actual maximum value.

Secondly, we can rewrite the subproblem to replace the variable square $\left\|\boldsymbol{w}_{n,k}\right\|^2$ to be affine function by setting an auxiliary positive semidefinite matrix $\boldsymbol{W}_{\boldsymbol{n,k}} = \boldsymbol{w}_{n,k} \boldsymbol{w}_{n,k}^H$. Moreover, we define $\boldsymbol{W}_{\boldsymbol{k}} = [\boldsymbol{W}_{1,k}, \boldsymbol{W}_{2,k}, \dots, \boldsymbol{W}_{n,k}]$, $\overline{\boldsymbol{B}} = [\underbrace{\boldsymbol{B}, \boldsymbol{B}, \dots, \boldsymbol{B}}_{\boldsymbol{N}}]$ and $\overline{\boldsymbol{\Theta}} = [\underbrace{\boldsymbol{\Theta}, \boldsymbol{\Theta}, \dots, \boldsymbol{\Theta}}_{\boldsymbol{N}}]$, which can be used to simplify the subfix user n. Therefore, C1 and C4, which contain quadratic terms, can be written as its equivalent form using trace:

$$\text{C1}: \sum_{k=1}^{K} Tr(\boldsymbol{A}_k \boldsymbol{A}_k^H \boldsymbol{W}_k) \leq P_{max}, \tag{12}$$

$$\text{C4}: \tau_k \leq Tr(\overline{\boldsymbol{H}}_k^H \overline{\boldsymbol{H}}_k \boldsymbol{A}_k \boldsymbol{A}_k^H \boldsymbol{W}_k), \forall k. \tag{13}$$

In addition, C6 can be rewritten in a combination of $\boldsymbol{W}_{\boldsymbol{k}}$, $\boldsymbol{A}_k$, $\overline{\boldsymbol{B}}$ and $\overline{\boldsymbol{\Theta}}$ as it contains a summation of n users' product of matrix:

$$\sum_{k=1}^{K} \|\overline{\boldsymbol{B}}\overline{\boldsymbol{\Theta}}\boldsymbol{G}_r \boldsymbol{A}_k \overline{\boldsymbol{W}}_k\|^2 + \sigma_d^2 \|\boldsymbol{B}\boldsymbol{\Theta}\|^2 \leq P_A \tag{14}$$

Similar to C1 and C4, this is equivalent to:

$$\sum_{k=1}^{K} Tr(\overline{\boldsymbol{B}}\overline{\boldsymbol{B}}^H \overline{\boldsymbol{\Theta}}\overline{\boldsymbol{\Theta}}^H \boldsymbol{G}_r \boldsymbol{G}_r^H \boldsymbol{A}_k \boldsymbol{A}_k^H \boldsymbol{W}_k) + \sigma_d^2 \|\boldsymbol{B}\boldsymbol{\Theta}\|^2 \leq P_A \tag{15}$$

Besides, as the auxiliary positive semidefinite matrix $\boldsymbol{W}_k$ is utilized, we have to include two more constrains to guarantee the correct outcome:

$$rank(\boldsymbol{W}_k) \leq 1, \forall k, \tag{16}$$

$$\boldsymbol{W}_k \succcurlyeq 0, \forall k, \tag{17}$$

By proofing the tightness SDP relaxation is tight, we can remove the non-convex constraint $rank(\boldsymbol{W}_k) \leq 1$. The detail for proof step of SDR will be mentioned at appendix section. After the transformation of $\boldsymbol{W}_k$. The overall subproblem can be rewritten as:

P1: $$Maximize_{\boldsymbol{W}_k, \tau_k, \beta_k} \frac{\sum_{k=1}^{K} \log(\beta_k + \tau_k) - \log(\beta_k)}{\sum_{k=1}^{K} Tr(\boldsymbol{A}_k \boldsymbol{A}_k^H \boldsymbol{W}_k) + Pc + \sum_{k=1}^{K} Tr(\overline{\boldsymbol{B}}\overline{\boldsymbol{B}}^H \overline{\boldsymbol{\Theta}}\overline{\boldsymbol{\Theta}}^H \boldsymbol{G}_r \boldsymbol{G}_r^H \boldsymbol{A}_k \boldsymbol{A}_k^H \boldsymbol{W}_k) + \sigma_d^2 \|\boldsymbol{B}\boldsymbol{\Theta}\|^2}$$

s.t $$\text{C1}: \sum_{k=1}^{K} Tr(\boldsymbol{A}_k \boldsymbol{A}_k^H \boldsymbol{W}_k) \leq P_{max}, \tag{18.1}$$

$$\text{C2}: \sum_{k=1}^{K} a_{n,k}(\log(\beta_k + \tau_k) - \log(\beta_k)) \leq C_n, \forall n, \tag{18.2}$$

$$\text{C3}: \log(\beta_k + \tau_k) - \log(\beta_k) \geq R_{k,min}, \forall k, \tag{18.3}$$

$$\text{C4}: \tau_k \leq Tr(\overline{\boldsymbol{H}}_k^H \overline{\boldsymbol{H}}_k \boldsymbol{A}_k \boldsymbol{A}_k^H \boldsymbol{W}_k), \forall k, \tag{18.4}$$

$$\text{C5}: \beta_k \geq \sum_{j \neq k}^{K} \left|\overline{\boldsymbol{H}}_j^H \boldsymbol{A}_j \boldsymbol{W}_j\right|^2 + \sigma_d^2 \left\|\boldsymbol{H}_{r,k}^H \boldsymbol{B}\boldsymbol{\Theta}\right\|^2 + \sigma_{n_k}^2, \forall k, \tag{18.5}$$

$$C6: \boldsymbol{W}_k \succcurlyeq 0, \forall k, \tag{18.6}$$

$$\text{C7}: \sum_{k=1}^{K} Tr(\overline{\boldsymbol{B}}\overline{\boldsymbol{B}}^H \overline{\boldsymbol{\Theta}}\overline{\boldsymbol{\Theta}}^H \boldsymbol{G}_r \boldsymbol{G}_r^H \boldsymbol{A}_k \boldsymbol{A}_k^H \boldsymbol{W}_k) + \sigma_d^2 \|\boldsymbol{B}\boldsymbol{\Theta}\|^2 \leq P_A. \tag{18.7}$$

So far, it can be observed that the objective function, constrain C2 and C3 are still non-convex, as it contains a concave function $\log(\beta_k + \tau_k)$ subtract another concave function $\log(\beta_k)$. In order to guarantee the convexity, our design considers the application of Success Convex Approximation (SCA) method. As both the $\log(\beta_k + \tau_k)$ and $\log(\beta_k)$ are concave function, we use SCA to find the upper bound $C_1^{(t)} \geq \log(\beta_k)$ for each user. Then $Maximize \log(\beta_k + \tau_k) - C_1^{(t)}$ becomes a convex function. In terms of C2, we use SCA to find the upper bound $C_2^{(t)} \geq \log(\beta_k + \tau_k)$.

Both the upper bound $C_1^{(t)}$ and $C_2^{(t)}$ can be obtained by applying the second order Tylor expansion [54]. It can be written as:

$$f(x) \leq f\left(x^{(t)}\right) + f'\left(x^{(t)}\right)\left(x - x^{(t)}\right) \tag{19}$$

After we substitute the $\log(\beta_k + \tau_k)$ and $\log(\beta_k)$ into the Tylor expansion, it becomes:

$$\log(\beta_k + \tau_k) \leq \log(\beta_k^t + \tau_k^t) + \frac{1}{(\beta_k^t + \tau_k^t)\ln(2)}(\beta_k + \tau_k - \beta_k^t - \tau_k^t) = C_2^{(t)}, \quad (20)$$

$$\log(\beta_k) \leq \log(\beta_k^t) + \frac{1}{\beta_k^t \ln(2)}(\beta_k - \beta_k^t) = C_1^{(t)}, \quad (21)$$

where the β_k^t and τ_k^t are variables value of β_k and τ_k at the t-th iteration. The inequality will become equality when β_k^t and τ_k^t are exactly equal to β_k and τ_k.

After SCA, the subproblem becomes:

$$\text{P1:} \quad Maximize_{\boldsymbol{W}_k, \tau_k, \beta_k} \frac{\sum_{k=1}^{K}(C_2^{(t)} - C_1^{(t)})}{\sum_{k=1}^{K} Tr(\boldsymbol{A}_k \boldsymbol{A}_k^H \boldsymbol{W}_k) + Pc + \sum_{k=1}^{K} Tr(\overline{\boldsymbol{B}}\overline{\boldsymbol{B}}^H \overline{\boldsymbol{\Theta}}\overline{\boldsymbol{\Theta}}^H \boldsymbol{G}_r \boldsymbol{G}_r^H \boldsymbol{A}_k \boldsymbol{A}_k^H \boldsymbol{W}_k) + \sigma_d^2 \|\boldsymbol{B}\boldsymbol{\Theta}\|^2}$$

$$\text{s.t} \quad \text{C1:} \sum_{k=1}^{K} Tr(\boldsymbol{A}_k \boldsymbol{A}_k^H \boldsymbol{W}_k) \leq P_{max}, \quad (22.1)$$

$$\text{C2:} \sum_{k=1}^{K} a_{n,k}(C_2^{(t)} - C_1^{(t)}) \leq C_n, \forall n, \quad (22.2)$$

$$\text{C3:} C_2^{(t)} - C_1^{(t)} \geq R_{k,min}, \forall k, \quad (22.3)$$

$$\text{C4:} \tau_k \leq Tr(\overline{\boldsymbol{H}}_k^H \overline{\boldsymbol{H}}_k \boldsymbol{A}_k \boldsymbol{A}_k^H \boldsymbol{W}_k), \forall k, \quad (22.4)$$

$$\text{C5:} \beta_k \geq \sum_{j \neq k}^{K} \left|\overline{\boldsymbol{H}}_j^H \boldsymbol{A}_j \boldsymbol{W}_j\right|^2 + \sigma_d^2 \left\|\boldsymbol{H}_{r,k}^H \boldsymbol{B}\boldsymbol{\Theta}\right\|^2 + \sigma_{n_k}^2, \forall k, \quad (22.5)$$

$$C6: \boldsymbol{W}_k \succcurlyeq 0, \forall k, \quad (22.6)$$

$$\text{C7:} \sum_{k=1}^{K} Tr(\overline{\boldsymbol{B}}\overline{\boldsymbol{B}}^H \overline{\boldsymbol{\Theta}}\overline{\boldsymbol{\Theta}}^H \boldsymbol{G}_r \boldsymbol{G}_r^H \boldsymbol{A}_k \boldsymbol{A}_k^H \boldsymbol{W}_k) + \sigma_d^2 \|\boldsymbol{B}\boldsymbol{\Theta}\|^2 \leq P_A. \quad (22.7)$$

Therefore, it can be seen that all the constraints are convex. However, the objective function is still a fractional quasi-convex function. We can handle the objective function using Dinkelbach method. It can transform the ratio of two linear fractional programming $\max\{\frac{N(x)}{D(x)} | x \in S\}$ to a convex programming $F(q_k) = \max\{N(x) - q_k D(x) | x \in S\}$ [55], where q_k will get updated and approach to the maximum value while $F(q_k)$ getting closer to 0 in each iteration. The optimal value will be found when $F(q_k)$ becomes less than a predefined optimality tolerance which is close to 0. According to the Dinkelbach method, our objective function can be formulated as:

$$Maximize_{\boldsymbol{W}_k,\tau_k,\beta_k} \frac{\sum_{k=1}^{K}(C_2^{(t)}-C_1^{(t)})}{\sum_{k=1}^{K} Tr(\boldsymbol{A}_k\boldsymbol{A}_k^H\boldsymbol{W}_k)+Pc+\sum_{k=1}^{K} Tr(\overline{\boldsymbol{B}}\overline{\boldsymbol{B}}^H\overline{\boldsymbol{\Theta}}\overline{\boldsymbol{\Theta}}^H\boldsymbol{G}_r\boldsymbol{G}_r^H\boldsymbol{A}_k\boldsymbol{A}_k^H\boldsymbol{W}_k)+\sigma_d^2\|\boldsymbol{B}\boldsymbol{\Theta}\|^2} \leftrightarrow$$

$$Maximize_{\boldsymbol{W}_k,\tau_k,\beta_k} \sum_{k=1}^{K}(C_2^{(t)} - C_1^{(t)}) - q^*\Big[\sum_{k=1}^{K} Tr\big(\boldsymbol{A}_k\boldsymbol{A}_k^H\boldsymbol{W}_k\big) + Pc +$$

$$\sum_{k=1}^{K} Tr\Big(\overline{\boldsymbol{B}}\overline{\boldsymbol{B}}^H\overline{\boldsymbol{\Theta}}\overline{\boldsymbol{\Theta}}^H\boldsymbol{G}_r\boldsymbol{G}_r^H\boldsymbol{A}_k\boldsymbol{A}_k^H\boldsymbol{W}_k\Big) + \sigma_d^2\big\|\boldsymbol{B}\boldsymbol{\Theta}\big\|^2\Big] \quad (23)$$

Therefore, the final version of subproblem1 becomes:

P1: $Minimize_{\boldsymbol{W}_k,\tau_k,\beta_k} - \sum_{k=1}^{K}(C_2^{(t)} - C_1^{(t)}) + q^*\Big[\sum_{k=1}^{K} Tr(\boldsymbol{A}_k\boldsymbol{A}_k^H\boldsymbol{W}_k) + Pc +$

$\sum_{k=1}^{K} Tr(\overline{\boldsymbol{B}}\overline{\boldsymbol{B}}^H\overline{\boldsymbol{\Theta}}\overline{\boldsymbol{\Theta}}^H\boldsymbol{G}_r\boldsymbol{G}_r^H\boldsymbol{A}_k\boldsymbol{A}_k^H\boldsymbol{W}_k) + \sigma_d^2\big\|\boldsymbol{B}\boldsymbol{\Theta}\big\|^2\Big]$

s.t $\quad C1: \sum_{k=1}^{K} Tr(\boldsymbol{A}_k\boldsymbol{A}_k^H\boldsymbol{W}_k) \le P_{max}, \quad (24.1)$

$C2: \sum_{k=1}^{K} a_{n,k}(C_2^{(t)} - C_1^{(t)}) \le C_n, \forall n, \quad (24.2)$

$C3: C_2^{(t)} - C_1^{(t)} \ge R_{k,min}, \forall k, \quad (24.3)$

$C4: \tau_k \le Tr(\overline{\boldsymbol{H}}_k^H\overline{\boldsymbol{H}}_k\boldsymbol{A}_k\boldsymbol{A}_k^H\boldsymbol{W}_k), \forall k, \quad (24.4)$

$C5: \beta_k \ge \sum_{j\ne k}^{K}\big|\overline{\boldsymbol{H}}_j^H\boldsymbol{A}_j\boldsymbol{W}_j\big|^2 + \sigma_d^2\big\|\boldsymbol{H}_{r,k}^H\boldsymbol{B}\boldsymbol{\Theta}\big\|^2 + \sigma_{n_k}^2, \forall k, \quad (24.5)$

$C6: \boldsymbol{W}_k \succcurlyeq 0, \forall k, \quad (24.6)$

$C7: \sum_{k=1}^{K} Tr(\overline{\boldsymbol{B}}\overline{\boldsymbol{B}}^H\overline{\boldsymbol{\Theta}}\overline{\boldsymbol{\Theta}}^H\boldsymbol{G}_r\boldsymbol{G}_r^H\boldsymbol{A}_k\boldsymbol{A}_k^H\boldsymbol{W}_k) + \sigma_d^2\|\boldsymbol{B}\boldsymbol{\Theta}\|^2 \le P_A. \quad (24.7)$

The algorithm for subproblem beamforming optimization applying SCA and Dinkelbach method is shown below:

Algorithm 1. Alternating optimization of $\boldsymbol{W}_k$

---

1. **Initialize** $\boldsymbol{B} = \boldsymbol{B_0}$ and $\boldsymbol{\Theta} = \boldsymbol{\Theta_0}$, set the first iteration index $t = 0, \beta_k^t = \beta_0, \tau_k^t = \tau_0$.
2. **Repeat**
3. Initialize second iteration index $j = 0$. Using provided β_k^t and τ_k^t to solve SCA upper bound $C^{(t)}$ and solve $\boldsymbol{W}_k$.
4. **Repeat**
5. Initialize $q^* = 0$, solving Dinkelbach objective function and finding the maximum value q^*

6. $j = j + 1$
7. **Until** $F(q_k)$ less than optimality tolerance
8. **Update** $\beta_k^t = \beta_k,\ \tau_k^t = \tau_k$ and $t = t + 1$
9. **Until** convergence
10. Output the optimal solution $\boldsymbol{W_k^* = W}_k$

4.2 Subproblem 2: Amplitude matrix $\boldsymbol{B}$ optimization

In terms of subproblem 2 we set $\boldsymbol{B}$ as the optimization variable while $\boldsymbol{W}_k$ and $\boldsymbol{\Theta}$ are fixed. The problem P2 can be written as:

$$P2: Maximize_{\boldsymbol{B},\tau_k,\beta_k} \frac{\sum_{k=1}^{K}(\log(\beta_k + \tau_k) - \log(\beta_k))}{\sum_{k=1}^{K} Tr(\boldsymbol{A}_k\boldsymbol{A}_k^H\boldsymbol{W}_k) + Pc + \sum_{k=1}^{K} Tr(\overline{\boldsymbol{B}}\overline{\boldsymbol{B}}^H\overline{\boldsymbol{\Theta}}\overline{\boldsymbol{\Theta}}^H\boldsymbol{G}_r\boldsymbol{G}_r^H\boldsymbol{A}_k\boldsymbol{A}_k^H\boldsymbol{W}_k) + \sigma_d^2\|\boldsymbol{B\Theta}\|^2}$$

$$\text{s.t}\quad \text{C1}: \sum_{k=1}^{K} a_{n,k}\ (\log(\beta_k + \tau_k) - \log(\beta_k)) \le C_n, \forall n, \tag{25.1}$$

$$\text{C2}: \log(\beta_k + \tau_k) - \log(\beta_k) \ge R_{k,min}, \forall k, \tag{25.2}$$

$$\text{C3}: \tau_k \le |\overline{\boldsymbol{H}}_k^H\boldsymbol{A}_k\overline{\boldsymbol{W}}_k|^2, \forall k, \tag{25.3}$$

$$\text{C4}: \beta_k \ge \sum_{j\ne k}^{K}\left|\overline{\boldsymbol{H}}_k^H\boldsymbol{A}_j\overline{\boldsymbol{W}}_j\right|^2 + \sigma_d^2\left\|\boldsymbol{H}_{r,k}^H\boldsymbol{B\Theta}\right\|^2 + \sigma_{n_k}^2, \forall k, \tag{25.4}$$

$$\text{C5}: \sum_{k=1}^{K} Tr(\overline{\boldsymbol{B}}\overline{\boldsymbol{B}}^H\overline{\boldsymbol{\Theta}}\overline{\boldsymbol{\Theta}}^H\boldsymbol{G}_r\boldsymbol{G}_r^H\boldsymbol{A}_k\boldsymbol{A}_k^H\boldsymbol{W}_k) + \sigma_d^2\|\boldsymbol{B\Theta}\|^2 \le P_A. \tag{25.5}$$

In problem P2, the objective function and C3 are non-convex. In C3 we have $|\overline{\boldsymbol{H}}_k^H\boldsymbol{A}_k\overline{\boldsymbol{W}}_k|^2$. As we know that $\overline{\boldsymbol{H}}_{n,k} = \boldsymbol{h}_{n,k} + \boldsymbol{h}_{r,k}\boldsymbol{B\Theta G}_{n,r}$ and $\overline{\boldsymbol{H}}_k = [\overline{\boldsymbol{H}}_{1,k}, \overline{\boldsymbol{H}}_{2,k}, \dots, \overline{\boldsymbol{H}}_{n,k}]$, we can simplify the C3 to be equivalent form:

$$\tau_k \le |\overline{\boldsymbol{H}}_k^H\boldsymbol{A}_k\overline{\boldsymbol{W}}_k|^2 = |(\boldsymbol{h}^H + \boldsymbol{v\varphi})\boldsymbol{A}_k\overline{\boldsymbol{W}}_k|^2 = |\boldsymbol{h}^H\boldsymbol{A}_k\overline{\boldsymbol{W}}_k + \boldsymbol{v}^H\boldsymbol{\varphi A}_k\overline{\boldsymbol{W}}_k|^2 =$$
$$|\boldsymbol{H}^H + \boldsymbol{v}^H\emptyset|^2 = \overline{\boldsymbol{v}}^H\boldsymbol{R}\overline{\boldsymbol{v}}, \tag{26}$$

where we firstly define $\boldsymbol{h}^H = [\boldsymbol{h}_{1,k}^H, \boldsymbol{h}_{2,k}^H, \dots, \boldsymbol{h}_{n,k}^H]$, $\boldsymbol{v}^H = [\beta_1, \beta_2, \dots, \beta_M, \beta_1, \beta_2, \dots, \beta_M, \beta_1, \beta_2, \dots, \beta_M]$ which repeat K times. To further simplify the formular, we set $\boldsymbol{H}^H = \boldsymbol{h}^H\boldsymbol{A}_k\overline{\boldsymbol{W}}_k$ and $\emptyset = \boldsymbol{\varphi A}_k\overline{\boldsymbol{W}}_k$. Then we try to write the formular in quadratic form $\overline{\boldsymbol{v}}^H\boldsymbol{R}\overline{\boldsymbol{v}}$ where $\overline{\boldsymbol{v}} = \begin{bmatrix}\boldsymbol{v}\\1\end{bmatrix}$ and $R =$

$\begin{bmatrix} \emptyset\emptyset^{\boldsymbol{H}} & \emptyset\boldsymbol{H} \\ \boldsymbol{H}^H\emptyset & 0 \end{bmatrix}$. In addition, we know that $\overline{\boldsymbol{v}}^{\boldsymbol{H}}\boldsymbol{R}\overline{\boldsymbol{v}} = \boldsymbol{Tr}(\boldsymbol{R}\overline{\boldsymbol{v}}\overline{\boldsymbol{v}}^{\boldsymbol{H}})$ and we can set positive semidefinite matrix $\boldsymbol{V} = \overline{\boldsymbol{v}}\overline{\boldsymbol{v}}^{\boldsymbol{H}}$. Therefore, we can write $\tau_k \leq \boldsymbol{Tr}(\boldsymbol{RV})$. Finally, the subproblem P2 can be formulated as:

$$Maximize_{\boldsymbol{B},\boldsymbol{V},\tau_k,\beta_k} \frac{\sum_{k=1}^{K}\left(\log\left(\beta_k+\tau_k\right)-\log\left(\beta_k\right)\right)}{\sum_{k=1}^{K} Tr(\boldsymbol{A}_k\boldsymbol{A}_k^H\boldsymbol{W}_k)+Pc+\sum_{k=1}^{K} Tr(\overline{\boldsymbol{B}}\overline{\boldsymbol{B}}^H\overline{\boldsymbol{\Theta}}\overline{\boldsymbol{\Theta}}^H\boldsymbol{G}_r\boldsymbol{G}_r^H\boldsymbol{A}_k\boldsymbol{A}_k^H\boldsymbol{W}_k)+\sigma_d^2\|\boldsymbol{B}\boldsymbol{\Theta}\|^2}$$

s.t C1: $\sum_{k=1}^{K} a_{n,k}\ (\log(\beta_k+\tau_k)-\log(\beta_k)) \leq C_n, \forall n,$ (27.1)

C2: $\log(\beta_k+\tau_k)-\log(\beta_k) \geq R_{k,min}, \forall k,$ (27.2)

C3: $\tau_k \leq \boldsymbol{Tr}(\boldsymbol{RV}), \forall k,$ (27.3)

C4: $\beta_k \geq \sum_{j\neq k}^{K}\left|\overline{\boldsymbol{H}}_k^H\boldsymbol{A}_j\overline{\boldsymbol{W}}_j\right|^2+\sigma_d^2\left\|\boldsymbol{H}_{r,k}^H\boldsymbol{B}\boldsymbol{\Theta}\right\|^2+\sigma_{n_k}^2, \forall k,$ (27.4)

C5: $\sum_{k=1}^{K} Tr(\overline{\boldsymbol{B}}\overline{\boldsymbol{B}}^H\overline{\boldsymbol{\Theta}}\overline{\boldsymbol{\Theta}}^H\boldsymbol{G}_r\boldsymbol{G}_r^H\boldsymbol{A}_k\boldsymbol{A}_k^H\boldsymbol{W}_k)+\sigma_d^2\|\boldsymbol{B}\boldsymbol{\Theta}\|^2 \leq P_A.$ (27.5)

C6: $\boldsymbol{V} = \overline{\boldsymbol{v}}\overline{\boldsymbol{v}}^{\boldsymbol{H}}$ (27.6)

C7: $\text{Rank}(\boldsymbol{V}) = 1$ (27.7)

C8: $\boldsymbol{V} \succcurlyeq 0$ (27.8)

By applying SDR is tight we can remove the constrain C7. Similarly, by applying SCA to $(\log(\beta_k+\tau_k)$ and $\log(\beta_k)$, the problem becomes:

$$Maximize_{\boldsymbol{B},\boldsymbol{V},\tau_k,\beta_k} \frac{C_2^{(t)}-C_1^{(t)}}{\sum_{k=1}^{K} Tr(\boldsymbol{A}_k\boldsymbol{A}_k^H\boldsymbol{W}_k)+Pc+\sum_{k=1}^{K} Tr(\overline{\boldsymbol{B}}\overline{\boldsymbol{B}}^H\overline{\boldsymbol{\Theta}}\overline{\boldsymbol{\Theta}}^H\boldsymbol{G}_r\boldsymbol{G}_r^H\boldsymbol{A}_k\boldsymbol{A}_k^H\boldsymbol{W}_k)+\sigma_d^2\|\boldsymbol{B}\boldsymbol{\Theta}\|^2}$$

s.t C1: $\sum_{k=1}^{K} a_{n,k}(C_2^{(t)}-C_1^{(t)}) \leq C_n, \forall n,$ (28.1)

C2: $C_2^{(t)}-C_1^{(t)} \geq R_{k,min}, \forall k,$ (28.2)

C3: $\tau_k \leq \boldsymbol{Tr}(\boldsymbol{RV}), \forall k,$ (28.3)

C4: $\beta_k \geq \sum_{j\neq k}^{K}\left|\overline{\boldsymbol{H}}_k^H\boldsymbol{A}_j\boldsymbol{W}_j\right|^2+\sigma_d^2\left\|\boldsymbol{H}_{r,k}^H\boldsymbol{B}\boldsymbol{\Theta}\right\|^2+\sigma_{n_k}^2, \forall k,$ (28.4)

C5: $\sum_{k=1}^{K} Tr(\overline{\boldsymbol{B}}\overline{\boldsymbol{B}}^H\overline{\boldsymbol{\Theta}}\overline{\boldsymbol{\Theta}}^H\boldsymbol{G}_r\boldsymbol{G}_r^H\boldsymbol{A}_k\boldsymbol{A}_k^H\boldsymbol{W}_k)+\sigma_d^2\|\boldsymbol{B}\boldsymbol{\Theta}\|^2 \leq P_A.$ (28.5)

C6: $\boldsymbol{V} = \overline{\boldsymbol{v}}\overline{\boldsymbol{v}}^{\boldsymbol{H}}$ (28.6)

C7: $\boldsymbol{V} \succcurlyeq 0$ (28.7)

Similarly, the problem can be solved using Dinkelbach method.

$$P2: Minimize_{\boldsymbol{W}_k,\tau_k,\beta_k} -C_2^{(t)}+C_1^{(t)}+q^*\left[\sum_{k=1}^{K} Tr(\boldsymbol{A}_k\boldsymbol{A}_k^H\boldsymbol{W}_k)+Pc+\right.$$

$\sum_{k=1}^{K} Tr(\overline{\boldsymbol{B}}\overline{\boldsymbol{B}}^H\overline{\boldsymbol{\Theta}}\overline{\boldsymbol{\Theta}}^H\boldsymbol{G}_r\boldsymbol{G}_r^H\boldsymbol{A}_k\boldsymbol{A}_k^H\boldsymbol{W}_k) + \sigma_d^2\|\boldsymbol{B}\boldsymbol{\Theta}\|^2\Big]$

$$\text{s.t} \quad \text{C1}: \sum_{k=1}^{K} a_{n,k}(C_2^{(t)} - C_1^{(t)}) \le C_n\,, \forall n, \tag{29.1}$$

$$\text{C2}: C_2^{(t)} - C_1^{(t)} \ge R_{k,min}, \forall k, \tag{29.2}$$

$$\text{C3}: \tau_k \le \boldsymbol{Tr}(\boldsymbol{RV}), \forall k, \tag{29.3}$$

$$\text{C4}: \beta_k \ge \sum_{j\ne k}^{K}\left|\overline{\boldsymbol{H}}_k^H\boldsymbol{A}_j\boldsymbol{W}_j\right|^2 + \sigma_d^2\left\|\boldsymbol{H}_{r,k}^H\boldsymbol{B}\boldsymbol{\Theta}\right\|^2 + \sigma_{n_k}^2, \forall k, \tag{29.4}$$

$$\text{C5}: \sum_{k=1}^{K} Tr(\overline{\boldsymbol{B}}\overline{\boldsymbol{B}}^H\overline{\boldsymbol{\Theta}}\overline{\boldsymbol{\Theta}}^H\boldsymbol{G}_r\boldsymbol{G}_r^H\boldsymbol{A}_k\boldsymbol{A}_k^H\boldsymbol{W}_k) + \sigma_d^2\|\boldsymbol{B}\boldsymbol{\Theta}\|^2 \le P_A. \tag{29.5}$$

$$\text{C6}: \boldsymbol{V} = \overline{\boldsymbol{v}}\overline{\boldsymbol{v}}^{\boldsymbol{H}} \tag{29.6}$$

$$\text{C7}: \boldsymbol{V} \succcurlyeq 0 \tag{29.7}$$

Algorithm 2. Alternating optimization of $\boldsymbol{B}$ and $\boldsymbol{\Theta}$

---

1. **Initialize** $\boldsymbol{W}_k = \boldsymbol{W}_k^*$ and $\boldsymbol{\Theta} = \boldsymbol{\Theta_0}$, set the first iteration index $t = 0, \beta_k^t = \beta_0, \tau_k^t = \tau_0$.
2. **Repeat**
3. Initialize second iteration index $j = 0$. Using provided β_k^t and τ_k^t to solve SCA upper bound $C^{(t)}$ and solve $\boldsymbol{B}$.
4. **Repeat**
5. Initialize $q^* = 0$, solving Dinkelbach objective function and finding the maximum value q^*
6. $j = j + 1$
7. **Until** $F(q_k)$ less than optimality tolerance
8. **Update** $\beta_k^t = \beta_k,\ \tau_k^t = \tau_k$ and $t = t + 1$
9. **Until** convergence
10. Output the optimal solution $\boldsymbol{B}^* = \boldsymbol{B}$

Similar to subproblem of $\boldsymbol{B}$, subproblem P3 with changing variable $\boldsymbol{\Theta}$ can also be written as follows:

$P3: Minimize_{\boldsymbol{W}_k,\tau_k,\beta_k} - C_2^{(t)} + C_1^{(t)} + q^*\Big[\sum_{k=1}^{K} Tr(\boldsymbol{A}_k\boldsymbol{A}_k^H\boldsymbol{W}_k) + Pc +$

$\sum_{k=1}^{K} Tr(\overline{\boldsymbol{B}}\overline{\boldsymbol{B}}^H\overline{\boldsymbol{\Theta}}\overline{\boldsymbol{\Theta}}^H\boldsymbol{G}_r\boldsymbol{G}_r^H\boldsymbol{A}_k\boldsymbol{A}_k^H\boldsymbol{W}_k) + \sigma_d^2\|\boldsymbol{B}\boldsymbol{\Theta}\|^2\big]$

$$\text{s.t} \quad \text{C1}: \sum_{k=1}^{K} a_{n,k}(C_2^{(t)} - C_1^{(t)}) \le C_n\,, \forall n, \tag{30.1}$$

$$\text{C2}: C_2^{(t)} - C_1^{(t)} \ge R_{k,min}, \forall k, \tag{30.2}$$

$$\text{C3}: \tau_k \le \boldsymbol{Tr}(\boldsymbol{RV}), \forall k, \tag{30.3}$$

$$\text{C4}: \beta_k \ge \sum_{j\ne k}^{K}\left|\overline{\boldsymbol{H}}_k^H\boldsymbol{A}_j\boldsymbol{W}_j\right|^2 + \sigma_d^2\left\|\boldsymbol{H}_{r,k}^H\boldsymbol{B}\boldsymbol{\Theta}\right\|^2 + \sigma_{n_k}^2, \forall k, \tag{30.4}$$

$$\text{C5}: \sum_{k=1}^{K} Tr(\overline{\boldsymbol{B}}\overline{\boldsymbol{B}}^H\overline{\boldsymbol{\Theta}}\overline{\boldsymbol{\Theta}}^H\boldsymbol{G}_r\boldsymbol{G}_r^H\boldsymbol{A}_k\boldsymbol{A}_k^H\boldsymbol{W}_k) + \sigma_d^2\|\boldsymbol{B}\boldsymbol{\Theta}\|^2 \le P_A. \tag{30.5}$$

$$\text{C6}: \boldsymbol{V} = \overline{\boldsymbol{v}}\overline{\boldsymbol{v}}^{\boldsymbol{H}} \tag{30.6}$$

$$\text{C7}: \boldsymbol{V} \succcurlyeq 0 \tag{30.7}$$

$$\text{C8}: 0 \le \theta_m \le 2\pi, \forall m, \tag{30.8}$$

The only difference between phase and amplitude optimization is that phase optimization has to be in $[0, 2\pi]$ range, which is included as constraint C8. Other optimization steps are exactly the same as amplitude optimization. The algorithm for phase optimization is shown below:

Algorithm 3. Alternating optimization of $\boldsymbol{\Theta}$

1. **Initialize** $\boldsymbol{W}_k = \boldsymbol{W}_{\boldsymbol{k}}^*$ and $\boldsymbol{B} = \boldsymbol{B}^*$, set the first iteration index $t = 0, \beta_k^t = \beta_0, \tau_k^t = \tau_0$.
2. **Repeat**
3. Initialize second iteration index $j = 0$. Using provided β_k^t and τ_k^t to solve SCA upper bound $C^{(t)}$ and solve $\boldsymbol{\Theta}$.
4. **Repeat**
5. Initialize $q^* = 0$, solving Dinkelbach objective function and finding the maximum value q^*
6. $j = j + 1$
7. **Until** $F(q_k)$ less than optimality tolerance
8. **Update** $\beta_k^t = \beta_k$, $\tau_k^t = \tau_k$ and $t = t + 1$
9. **Until** convergence

10. Output the optimal solution $\boldsymbol{\Theta}^* = \boldsymbol{\Theta}$

5 Simulation results

In order to simulate the system performance of energy efficiency, we consider an IRS-aided system with two users and two BSs. The distance between two BSs is 150 meters. The location of IRS is set at the middle of two BSs (75 meters to each BS). Users are distributed randomly around the IRS inside a 50 meters circle area. In terms of the large scale fading, we set the pass loss exponents of BS-IRS and IRS-users to be 2 and 3.6. For small scale fading, we consider the IRS reflected path to be independent and Rician distribution, which is set to be 6dB. The maximum allowance power for BS P_{max} and for IRS P_A are both set to be 30 dBm. The backhaul capacity C_n is 10 bit/s/Hz. In addition, the optimality tolerance used in iteration of Dinkelbach method is 10^{-4}.

Firstly, in order to illustrate the influence of the number of IRS elements to the energy efficiency, we implemented the algorithm by adjusting the number of IRS elements from 50 to 500. In addition, to find out the relationship between energy efficiency and the number of BS antennas, we set N_t to be 3,6,9 and simulated respectively. The simulation results are shown in figure 7. As we can see, with the increase of IRS elements, the average system energy efficiency is slightly increased. For example, when $N_t = 3$, the energy efficiency starts with 5 Mbit/Joule at 50 IRS elements and ends with around 5.4 Mbit/Joule at 500 elements. This is reasonable as we increase the IRS element, the performance of IRS and the SINR will be enhanced. On the other hand, the total power is also increased because it requires larger power for IRS amplification with the increase of IRS elements. Therefore, the average energy efficiency does not increase dramatically with the number of IRS elements increasing. In terms of the number of BS antennas, the average energy

efficiency has a great improvement with more antennas. It is about 2.5 Mbit/Joule improvement of system energy efficiency when $N_t = 3$ changed to $N_t = 6$ at 50 IRS elements. Additional antennas can provide better information capacity and by calculating beamforming vector the power can be assigned wisely to each antenna. In our system design, increase the number of BS antennas can effectively improve the energy efficiency.

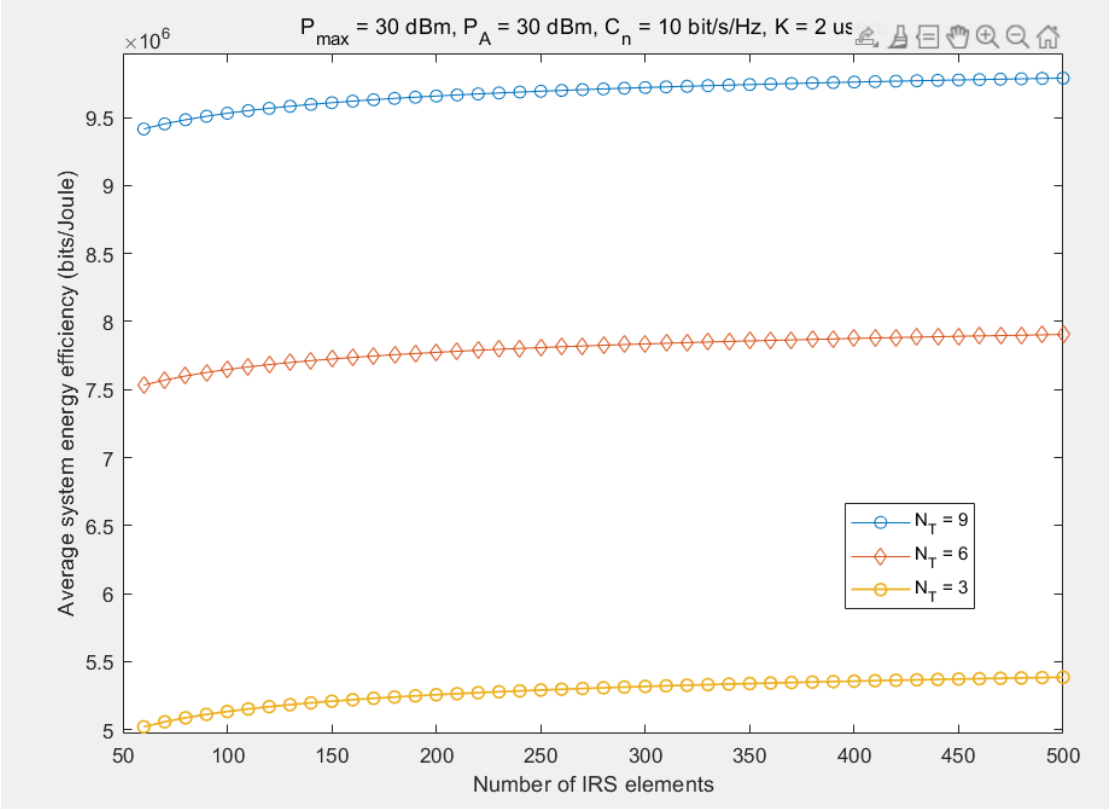

Figure 7. Average system energy efficiency versus number of IRS elements for different number of BS antennas ($N_t = 3,6,9$)

Secondly, we expect to evaluate the effectiveness of the proposed alternating optimization algorithm. One way to judge the algorithm performance is to show number of iterations required to converge. In figure 8, we plot the average energy efficiency versus the number of iterations with 60 IRS reflecting elements. It is observed that the average energy efficiency increases rapidly with the number of iterations. It shows that our algorithm has relatively good performance. For example, when $N_t = 3$, it takes only about 12 iterations for energy efficiency to be convergence. Moreover, the required number of

iterations for convergence increases with the number of BS antennas N_t. For instance, it takes about 13 iterations for $N_t = 6$ system to converge and 14 iterations for $N_t = 9$. It is acceptable as there are more variables in beamforming vector to deal with. Thus, we would need additional iterations for them to converge.

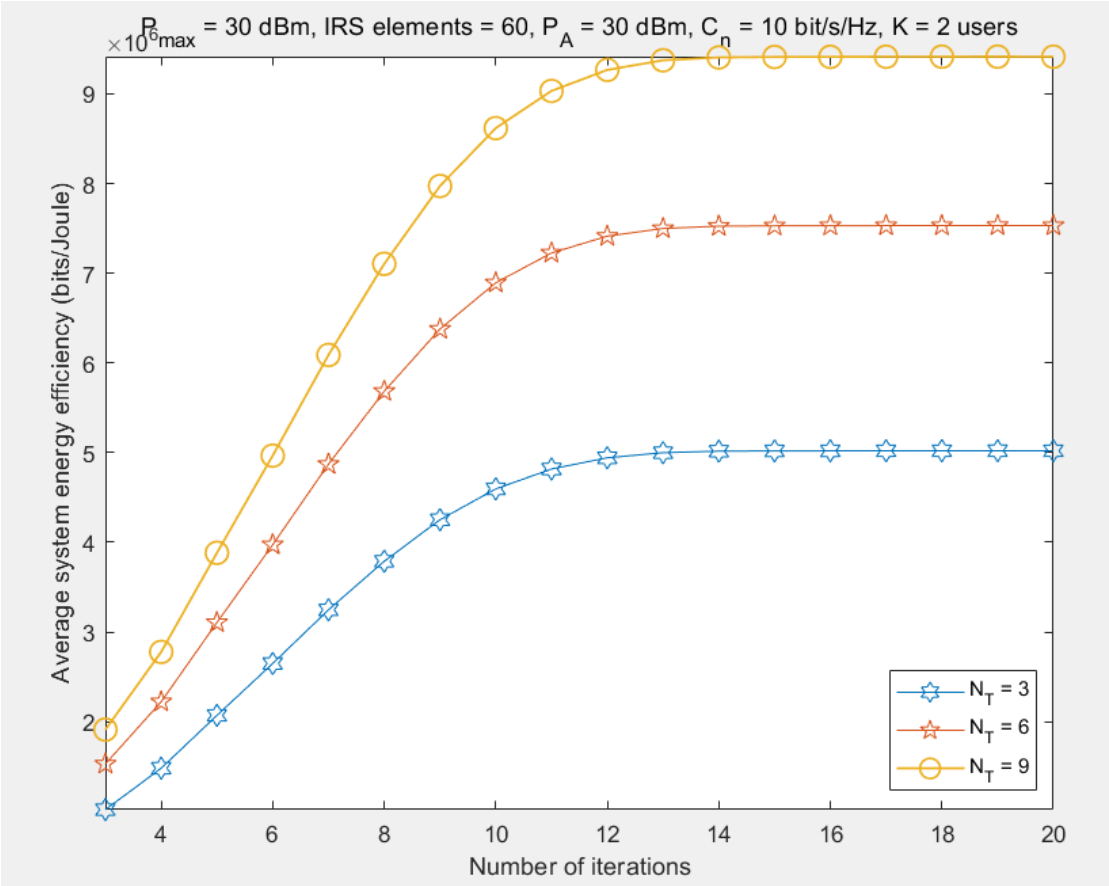

Figure 8. Average energy efficiency versus the number of iterations with 60 IRS reflecting elements

6 Conclusion

In this paper, we studied an energy-efficient beamforming for active IRS-aided JP-COMP downlink cell-edge multiuser MISO cellular network system. In order to enhance the quality of data transmission and energy efficiency, we applied JP-CoMP to reduce the cell-edge inter-cell interference and provide spatial

degree-of-freedom to CUs. In addition, active IRS is utilized to adjust both the amplitude and phase of IRS elements to achieve better beamforming and resource allocation. In terms of the algorithm design, we proposed a SCA, SDR and Dinkelbach method combined alternating optimization to provide a sub-optimal result for energy efficiency. It optimized the beamforming vector, amplitude matrix and phase shift matrix individually for each iteration, while others were fixed value obtained by last iteration.

Furthermore, we simulated and plotted the figures for both average system energy efficiency versus number of IRS elements and average energy efficiency versus the number of iterations for different number of BS antennas. It demonstrated that increase the number of IRS elements can slightly increase the average energy efficiency while adding extra BS antennas could dramatically increase the energy efficiency. Besides, we also illustrated that the proposed algorithm was efficient due to the relatively small number of iterations for the results to converge. The number of BS antenna could also increase the number of required iterations. Last but not least, further research can be conducted in the future to extend this paper’s content such as increasing the BS number and location, using multiple IRS, facing imperfect CSI, setting different value of backhaul capacity and so on.

7 Appendix

As mentioned in the problem solving section, the SDR is applied to remove the non-convex rank one constraint in (17). In order to proof the optimization problem to be convex and feasible, we need to make sure the slater's constraint and strong duality to be satisfied. We can construct a Lagrange dual function to prove the strong duality, which means the optimal value acquired from the dual problem must equal to the optimal value of primal problem. To prove the SDR is tight, KKT condition is used [56]-[58]. We derive the Lagrangian function to be:

$$
\begin{aligned}
&L(\boldsymbol{W}_k, \lambda1, \lambda2, \lambda3, \lambda4, \lambda5, \lambda6) \\
&= -\sum_{k=1}^{K}\left(C_2^{(t)} - C_1^{(t)}\right) + q^*\left[\sum_{k=1}^{K} Tr(\boldsymbol{A}_k\boldsymbol{A}_k^H\boldsymbol{W}_k) + Pc\right. \\
&\left. + \sum_{k=1}^{K} Tr(\bar{\boldsymbol{B}}\bar{\boldsymbol{B}}^H\bar{\boldsymbol{\Theta}}\bar{\boldsymbol{\Theta}}^H\boldsymbol{G}_r\boldsymbol{G}_r^H\boldsymbol{A}_k\boldsymbol{A}_k^H\boldsymbol{W}_k) + \sigma_d^2\|\boldsymbol{B}\boldsymbol{\Theta}\|^2\right] + \lambda1(Tr(\boldsymbol{A}_k\boldsymbol{A}_k^H\boldsymbol{W}_k) - P_{max}) \\
&+ \lambda2\left(\sum_{k=1}^{K} a_{n,k}\left(C_2^{(t)} - C_1^{(t)}\right) - C_n\right) + \lambda3\left(-C_2^{(t)} + C_1^{(t)} + R_{k,min}\right) \\
&+ \lambda4\left(\tau_k - Tr(\bar{\boldsymbol{H}}_k^H\bar{\boldsymbol{H}}_k\boldsymbol{A}_k\boldsymbol{A}_k^H\boldsymbol{W}_k)\right) \\
&+ \lambda5\left(\sum_{j\neq k}^{K}\left|\bar{\boldsymbol{H}}_k^H\boldsymbol{A}_j\boldsymbol{W}_j\right|^2 + \sigma_d^2\left\|\boldsymbol{H}_{r,k}^H\boldsymbol{B}\boldsymbol{\Theta}\right\|^2 + \sigma_{n_k}^2 - \beta_k\right) - Tr(\boldsymbol{Y}\boldsymbol{W}_k) \\
&+ \lambda6\left(\sum_{k=1}^{K} Tr(\bar{\boldsymbol{B}}\bar{\boldsymbol{B}}^H\bar{\boldsymbol{\Theta}}\bar{\boldsymbol{\Theta}}^H\boldsymbol{G}_r\boldsymbol{G}_r^H\boldsymbol{A}_k\boldsymbol{A}_k^H\boldsymbol{W}_k) + \sigma_d^2\|\boldsymbol{B}\boldsymbol{\Theta}\|^2 - P_A\right), \quad (31)
\end{aligned}
$$

where $\boldsymbol{Y} \succcurlyeq 0$ and $\lambda1, \lambda2, \lambda3, \lambda4, \lambda5, \lambda6 > 0$ are dual variables corresponding to the constraints C6,C1,C2,C3,C4,C5,C7. From it we can write the dual problem:

$$\max_{\boldsymbol{Y}, \lambda1, \lambda2, \lambda3, \lambda4, \lambda5, \lambda6} \inf_{\boldsymbol{W}_k} L$$

Then we focus on KKT conditions based on $\boldsymbol{W}_k$. The value of $\boldsymbol{Y}$ can be calculated by taking the derivative of the Lagrange function with respect to $\boldsymbol{W}_k$ and setting the gradient of Lagrange function to 0:

$$
\begin{aligned}
\frac{\partial L}{\partial \boldsymbol{W}_k} &= q^*(\boldsymbol{A}_k\boldsymbol{A}_k^H + \bar{\boldsymbol{B}}\bar{\boldsymbol{B}}^H\bar{\boldsymbol{\Theta}}\bar{\boldsymbol{\Theta}}^H\boldsymbol{G}_r\boldsymbol{G}_r^H\boldsymbol{A}_k\boldsymbol{A}_k^H) + \lambda1\boldsymbol{A}_k\boldsymbol{A}_k^H - \lambda4\bar{\boldsymbol{H}}_k^H\bar{\boldsymbol{H}}_k\boldsymbol{A}_k\boldsymbol{A}_k^H \\
&+ \lambda5\bar{\boldsymbol{H}}_k^H\bar{\boldsymbol{H}}_k\boldsymbol{A}_j\boldsymbol{A}_j^H - \boldsymbol{Y} + \lambda6\bar{\boldsymbol{B}}\bar{\boldsymbol{B}}^H\bar{\boldsymbol{\Theta}}\bar{\boldsymbol{\Theta}}^H\boldsymbol{G}_r\boldsymbol{G}_r^H\boldsymbol{A}_k\boldsymbol{A}_k^H, \quad (32)
\end{aligned}
$$

$$\boldsymbol{Y} = q^*(\boldsymbol{A}_k\boldsymbol{A}_k^H + \overline{\boldsymbol{B}}\overline{\boldsymbol{B}}^H\overline{\boldsymbol{\Theta}}\overline{\boldsymbol{\Theta}}^H\boldsymbol{G}_r\boldsymbol{G}_r^H\boldsymbol{A}_k\boldsymbol{A}_k^H) + \lambda 1\boldsymbol{A}_k\boldsymbol{A}_k^H - \lambda 4\overline{\boldsymbol{H}}_k^H\overline{\boldsymbol{H}}_k\boldsymbol{A}_k\boldsymbol{A}_k^H$$
$$+ \lambda 5\overline{\boldsymbol{H}}_k^H\overline{\boldsymbol{H}}_k\boldsymbol{A}_j\boldsymbol{A}_j^H + \lambda 6\overline{\boldsymbol{B}}\overline{\boldsymbol{B}}^H\overline{\boldsymbol{\Theta}}\overline{\boldsymbol{\Theta}}^H\boldsymbol{G}_r\boldsymbol{G}_r^H\boldsymbol{A}_k\boldsymbol{A}_k^H\,, \qquad (33)$$

where $\boldsymbol{I}$ is identical matrix.

From the KKT condition we have:

$$\boldsymbol{Y}\boldsymbol{W}_k = \boldsymbol{0}$$

We can rewrite the (33) by introducing new matrix $\boldsymbol{C}$ and $\boldsymbol{D}$:

$$\boldsymbol{Y} = \boldsymbol{C} - \boldsymbol{D} \qquad (34)$$

where $\boldsymbol{C} = q^*(\boldsymbol{A}_k\boldsymbol{A}_k^H + \overline{\boldsymbol{B}}\overline{\boldsymbol{B}}^H\overline{\boldsymbol{\Theta}}\overline{\boldsymbol{\Theta}}^H\boldsymbol{G}_r\boldsymbol{G}_r^H\boldsymbol{A}_k\boldsymbol{A}_k^H) + \lambda 1\boldsymbol{A}_k\boldsymbol{A}_k^H$ and $\boldsymbol{D} = -\lambda 4\overline{\boldsymbol{H}}_k^H\overline{\boldsymbol{H}}_k\boldsymbol{A}_k\boldsymbol{A}_k^H + \lambda 5\overline{\boldsymbol{H}}_k^H\overline{\boldsymbol{H}}_k\boldsymbol{A}_j\boldsymbol{A}_j^H + \lambda 6\overline{\boldsymbol{B}}\overline{\boldsymbol{B}}^H\overline{\boldsymbol{\Theta}}\overline{\boldsymbol{\Theta}}^H\boldsymbol{G}_r\boldsymbol{G}_r^H\boldsymbol{A}_k\boldsymbol{A}_k^H$. We assume $\boldsymbol{C}$ is a positive semi-definite matrix. For any eigenvector $\overline{\boldsymbol{v}} \neq 0$, $\overline{\boldsymbol{v}}^{\boldsymbol{H}}\boldsymbol{C}\overline{\boldsymbol{v}} \geq \boldsymbol{0}$. Set $\boldsymbol{V} = \overline{\boldsymbol{v}}^{\boldsymbol{H}}\overline{\boldsymbol{v}}$ and multiple it on both sides of (34) and take trace operation. We get:

$$Tr(\boldsymbol{Y}\boldsymbol{V}) = Tr(\boldsymbol{C}\boldsymbol{V}) - Tr(\boldsymbol{D}\boldsymbol{V})$$
$$= -Tr(\boldsymbol{D}\boldsymbol{V}) \qquad (35)$$

As $Tr(\boldsymbol{D}\boldsymbol{V})$ is greater than zero and $Tr(\boldsymbol{Y}\boldsymbol{V})$ is larger than or equal to zero, in order to make sure the equality is satisfied, $\boldsymbol{C}$ must be a positive definite matrix and $Rank(\boldsymbol{C}) = N_t$. According to the basic principle of rank inequality:

$$Rank(\boldsymbol{A} + \boldsymbol{B}) \geq Rank(\boldsymbol{A}) - Rank(\boldsymbol{B}),$$

We can get:

$$Rank(\boldsymbol{Y}) = Rank(-\boldsymbol{Y}) = Rank(-\boldsymbol{C} + \boldsymbol{D}) \geq Rank(-\boldsymbol{C}) - Rank(\boldsymbol{D}) \geq N_t - 1 (36)$$

[59] where the column of $\boldsymbol{W}_k$ belongs to members of $\boldsymbol{Y}$. Therefore, we can declare that $Rank(\boldsymbol{W}_k) \leq 1$ is satisfied.

8 Reference

[1] I. F. Akyildiz, A. Kak and S. Nie, "6G and Beyond: The Future of Wireless Communications Systems," in IEEE Access, vol. 8, pp. 133995-134030, 2020.

[2] N. Rajatheva et al., ‘‘White paper on broadband connectivity in 6G,’’ 2020, arXiv:2004.14247. [Online]. Available: http://arxiv.org/abs/2004.14247

[3] M. Latva-aho, K. Leppänen, F. Clazzer, and A. Munari, “Key drivers and research challenges for 6G ubiquitous wireless intelligence,” 6G Flagship, Univ. Oulu, Oulu, Finland, White Paper, 2019.

[4] Z. Zhang et al., “6G wireless networks: Vision, requirements, architecture, and key technologies,” IEEE Veh. Technol. Mag., vol. 14, no. 3, pp. 28–41, Sep. 2019.

[5] W. Saad, M. Bennis, and M. Chen, “A vision of 6G wireless systems: Applications, trends, technologies, and open research problems,” IEEE Netw., vol. 34, no. 3, pp. 134–142, May 2020.

[6] F. Tariq, M. R. A. Khandaker, K.-K. Wong, M. A. Imran, M. Bennis, and M. Debbah, “A speculative study on 6G,” IEEE Wireless Commun., vol. 27, no. 4, pp. 118–125, Aug. 2020.

[7] W. Saad, M. Bennis, and M. Chen, ‘‘A vision of 6G wireless systems: Applications, trends, technologies, and open research problems,’’ IEEE Netw., vol. 34, no. 3, pp. 134–142, May 2020.

[8] J. Zhang, E. Björnson, M. Matthaiou, D. W. K. Ng, H. Yang and D. J. Love, "Prospective Multiple Antenna Technologies for Beyond 5G," in IEEE Journal on Selected Areas in Communications, vol. 38, no. 8, pp. 1637-1660, Aug. 2020

[9] L. Lu, G. Y. Li, A. L. Swindlehurst, A. Ashikhmin, and R. Zhang, ‘‘An overview of massive MIMO: Benefits and challenges,” IEEE J. Sel. Topics Signal Process., vol. 8, no. 5, pp. 742–758, Oct. 2014.

[10] E. G. Larsson, O. Edfors, F. Tufvesson, and T. L. Marzetta, “Massive MIMO for next generation wireless systems,” IEEE Commun. Mag., vol. 52, no.

2, pp. 186–195, Feb. 2014.

[11] A. L. Swindlehurst, E. Ayanoglu, P. Heydari, and F. Capolino, “Millimeter-wave massive MIMO: The next wireless revolution?” IEEE Commun. Mag., vol. 52, no. 9, pp. 56–62, Sep. 2014.

[12] M. Kamel, W. Hamouda, and A. Youssef, “Ultra-dense networks: A survey,” IEEE Commun. Surveys Tuts., vol. 18, no. 4, pp. 2522–2545, 4th Quart., 2016.

[13] V. W. Wong, D. W. K. Ng, R. Schober, and L.-C. Wang, Key Technologies for 5G Wireless Systems. Cambridge, U.K.: Cambridge Univ. Press, 2017.

[14] X. Chen, D. Wing Kwan Ng, W. Yu, E. G. Larsson, N. Al-Dhahir, and R. Schober, “Massive access for 5G and beyond,” 2020, arXiv:2002.03491. [Online]. Available: http://arxiv.org/abs/2002.03491

[15] S. Zhang, Q. Wu, S. Xu, and G. Y. Li, “Fundamental green tradeoffs: Progresses, challenges, and impacts on 5G networks,” IEEE Commun. Surveys Tuts., vol. 19, no. 1, pp. 33–56, 1st Quart., 2017.

[16] Q. Wu, G. Y. Li, W. Chen, D. W. K. Ng, and R. Schober, “An overview of sustainable green 5G networks,” IEEE Wireless Commun., vol. 24, no. 4, pp. 72–80, Aug. 2017.

[17] E. G. Larsson, O. Edfors, F. Tufvesson and T. L. Marzetta, "Massive MIMO for next generation wireless systems," in IEEE Communications Magazine, vol. 52, no. 2, pp. 186-195, February 2014.

[18] W. Wang, L. Yang, A. Meng, Y. Zhan and D. W. K. Ng, "Resource Allocation for IRS-aided JP-CoMP Downlink Cellular Networks with Underlaying D2D Communications," in IEEE Transactions on Wireless Communications.

[19] J. Wang et al., "Interplay Between RIS and AI in Wireless Communications: Fundamentals, Architectures, Applications, and Open Research Problems," in IEEE Journal on Selected Areas in Communications, vol. 39, no. 8, pp. 2271-2288, Aug. 2021.

[20] D. Xu, V. Jamali, X. Yu, D. W. K. Ng and R. Schober, "Optimal Resource Allocation Design for Large IRS-Assisted SWIPT Systems: A Scalable

Optimization Framework," in IEEE Transactions on Communications, vol. 70, no. 2, pp. 1423-1441, Feb. 2022.

[21] E. Shi et al., "Wireless Energy Transfer in RIS-Aided Cell-Free Massive MIMO Systems: Opportunities and Challenges," in IEEE Communications Magazine, vol. 60, no. 3, pp. 26-32, March 2022.

[22] D. Xu, X. Yu, D. W. Kwan Ng and R. Schober, "Resource Allocation for Active IRS-Assisted Multiuser Communication Systems," 2021 55th Asilomar Conference on Signals, Systems, and Computers, 2021, pp. 113-119.

[23] Z. Zhang, L. Dai, X. Chen, C. Liu, F. Yang, R. Schober, and H. V. Poor, “Active RIS vs. passive RIS: Which will prevail in 6G?” arXiv:2103.15154, 2021.

[24] D. Gesbert, S. Hanly, H. Huang, S. Shamai, O. Simeone, and W. Yu, “Multi-cell MIMO cooperative networks: a new look at interference,” IEEE J. Select. Areas Commun., vol. 28, no. 9, pp. 1380–1480, Dec. 2010.

[25] R. Irmer, H. Droste, P. Marsch, M. Grieger, G. Fettweis, S. Brueck, H. P. Mayer, L. Thiele, and V. Jungnickel, “Coordinated multipoint: Concepts, performance, and field trial results,” IEEE Commun. Mag., vol. 49, no. 2, pp. 102–111, Fec. 2011.

[26] O. Tipmongkolsilp, S. Zaghloul, and A. Jukan, “The evolution of cellular backhaul technologies: current issues and future trends,” IEEE Commun. Surveys Tuts., vol. 13, no. 1, pp. 97–113, 1st Quart. 2011.

[27] N. Yu et al., “Light propagation with phase discontinuities: Generalized laws of reflection and refraction,” Science, vol. 334, no. 6054, pp. 333–337, Oct. 2011.

[28] H.-T. Chen, A. J. Taylor, and N. Yu, “A review of metasurfaces: Physics and applications,” Rep. Progr. Phys., vol. 79, p. 7, Jun. 2016.

[29] S. Gong et al., "Toward Smart Wireless Communications via Intelligent Reflecting Surfaces: A Contemporary Survey," in IEEE Communications Surveys & Tutorials, vol. 22, no. 4, pp. 2283-2314, Fourthquarter 2020.

[30] F. Liu et al., “Programmable metasurfaces: State of the art and prospects,”

in Proc. IEEE Int. Symp. Circuits Syst. (ISCAS), May 2018, pp. 1–5.

[31] D. Xu, X. Yu, Y. Sun, D. W. K. Ng, and R. Schober, “Resource allocation for IRS-assisted full-duplex cognitive radio systems,” to appear in IEEE Trans. Commun., 2020.

[32] X. Yu, D. Xu, D. W. K. Ng and R. Schober, "Power-Efficient Resource Allocation for Multiuser MISO Systems via Intelligent Reflecting Surfaces," GLOBECOM 2020 - 2020 IEEE Global Communications Conference, 2020, pp. 1-6.

[33] Z. Wei, X. Yu, D. W. K. Ng and R. Schober, "Resource Allocation for Simultaneous Wireless Information and Power Transfer Systems: A Tutorial Overview," in Proceedings of the IEEE, vol. 110, no. 1, pp. 127-149, Jan. 2022, doi: 10.1109/JPROC.2021.3120888.

[34] J. Liu, K. Xiong, Y. Lu, D. W. K. Ng, Z. Zhong and Z. Han, "Energy Efficiency in Secure IRS-Aided SWIPT," in IEEE Wireless Communications Letters, vol. 9, no. 11, pp. 1884-1888, Nov. 2020.

[35] A. Khalili, S. Zargari, Q. Wu, D. W. K. Ng and R. Zhang, "Multi-Objective Resource Allocation for IRS-Aided SWIPT," in IEEE Wireless Communications Letters, vol. 10, no. 6, pp. 1324-1328, June 2021.

[36] S. Hu, Z. Wei, Y. Cai, D. W. K. Ng and J. Yuan, "Sum-Rate Maximization for Multiuser MISO Downlink Systems with Self-sustainable IRS," GLOBECOM 2020 - 2020 IEEE Global Communications Conference, 2020, pp. 1-7.

[37] Y. Cai, Z. Wei, R. Li, D. W. K. Ng and J. Yuan, "Joint Trajectory and Resource Allocation Design for Energy-Efficient Secure UAV Communication Systems," in IEEE Transactions on Communications, vol. 68, no. 7, pp. 4536-4553, July 2020.

[38] Q. Wu et al., "A Comprehensive Overview on 5G-and-Beyond Networks With UAVs: From Communications to Sensing and Intelligence," in IEEE Journal on Selected Areas in Communications, vol. 39, no. 10, pp. 2912-2945, Oct. 2021, doi: 10.1109/JSAC.2021.3088681.

[39] Y. Sun, D. Xu, D. W. K. Ng, L. Dai and R. Schober, "Optimal 3D-Trajectory

Design and Resource Allocation for Solar-Powered UAV Communication Systems," in IEEE Transactions on Communications, vol. 67, no. 6, pp. 4281-4298, June 2019, doi: 10.1109/TCOMM.2019.2900630.

[40] Y. Cai, Z. Wei, S. Hu, C. Liu, D. W. K. Ng and J. Yuan, "Resource Allocation and 3D Trajectory Design for Power-Efficient IRS-Assisted UAV-NOMA Communications," in IEEE Transactions on Wireless Communications, 2022, doi: 10.1109/TWC.2022.3183300.

[41] D. Xu, X. Yu, Y. Sun, D. W. K. Ng and R. Schober, "Resource Allocation for Secure IRS-Assisted Multiuser MISO Systems," 2019 IEEE Globecom Workshops (GC Wkshps), 2019, pp. 1-6.

[42] X. Yu, D. Xu, Y. Sun, D. W. K. Ng and R. Schober, "Robust and Secure Wireless Communications via Intelligent Reflecting Surfaces," in IEEE Journal on Selected Areas in Communications, vol. 38, no. 11, pp. 2637-2652, Nov. 2020, doi: 10.1109/JSAC.2020.3007043.

[43] X. Yu, D. Xu, D. W. K. Ng and R. Schober, "IRS-Assisted Green Communication Systems: Provable Convergence and Robust Optimization," in IEEE Transactions on Communications, vol. 69, no. 9, pp. 6313-6329, Sept. 2021, doi: 10.1109/TCOMM.2021.3087794.

[44] S. Hu, Z. Wei, Y. Cai, C. Liu, D. W. K. Ng and J. Yuan, "Robust and Secure Sum-Rate Maximization for Multiuser MISO Downlink Systems With Self-Sustainable IRS," in IEEE Transactions on Communications, vol. 69, no. 10, pp. 7032-7049, Oct. 2021, doi: 10.1109/TCOMM.2021.3097140.

[45] Q. Qi, X. Chen and D. W. K. Ng, "Robust Beamforming for NOMA-Based Cellular Massive IoT With SWIPT," in IEEE Transactions on Signal Processing, vol. 68, pp. 211-224, 2020, doi: 10.1109/TSP.2019.2959246.

[46] Z. Wei, L. Yang, D. W. K. Ng, J. Yuan and L. Hanzo, "On the Performance Gain of NOMA Over OMA in Uplink Communication Systems," in IEEE Transactions on Communications, vol. 68, no. 1, pp. 536-568, Jan. 2020, doi: 10.1109/TCOMM.2019.2948343.

[47] X. Chen, R. Jia and D. W. K. Ng, "On the Design of Massive Non-

Orthogonal Multiple Access With Imperfect Successive Interference Cancellation," in IEEE Transactions on Communications, vol. 67, no. 3, pp. 2539-2551, March 2019, doi: 10.1109/TCOMM.2018.2884476.

[48] H. Niu, Z. Chu, F. Zhou, C. Pan, D. W. K. Ng and H. X. Nguyen, "Double Intelligent Reflecting Surface-Assisted Multi-User MIMO Mmwave Systems With Hybrid Precoding," in IEEE Transactions on Vehicular Technology, vol. 71, no. 2, pp. 1575-1587, Feb. 2022.

[49] C. Liu, X. Liu, D. W. K. Ng and J. Yuan, "Deep Residual Learning for Channel Estimation in Intelligent Reflecting Surface-Assisted Multi-User Communications," in IEEE Transactions on Wireless Communications, vol. 21, no. 2, pp. 898-912, Feb. 2022, doi: 10.1109/TWC.2021.3100148.

[50] Xu, W., Yang, Z., Ng, D.W., Levorato, M., Eldar, Y.C., & Debbah, M. (2022). Edge Learning for B5G Networks with Distributed Signal Processing: Semantic Communication, Edge Computing, and Wireless Sensing. ArXiv, abs/2206.00422.

[51] Q. Wu and R. Zhang, “Towards smart and reconfigurable environment: Intelligent reflecting surface aided wireless network,” IEEE Commun. Mag., vol. 58, no. 1, pp. 106–112, Jan. 2020.

[52] X. Yu, V. Jamali, D. Xu, D. W. K. Ng and R. Schober, "Smart and Reconfigurable Wireless Communications: From IRS Modeling to Algorithm Design," in IEEE Wireless Communications, vol. 28, no. 6, pp. 118-125, December 2021

[53] R. Irmer et al., "Coordinated multipoint: Concepts, performance, and field trial results," in IEEE Communications Magazine, vol. 49, no. 2, pp. 102-111, February 2011

[54] Z. Chen, W. Chen, X. Ma, Z. Li, Y. Chi and C. Han, "Taylor Expansion Aided Gradient Descent Schemes for IRS-Enabled Terahertz MIMO Systems," 2020 IEEE Wireless Communications and Networking Conference Workshops (WCNCW), 2020, pp. 1-7

[55] D. W. K. Ng, E. S. Lo and R. Schober, "Wireless Information and Power Transfer: Energy Efficiency Optimization in OFDMA Systems," in IEEE Transactions on Wireless Communications, vol. 12, no. 12, pp. 6352-6370, December 2013.

[56] Y. Gao, Q. Wu, G. Zhang, W. Chen, D. W. K. Ng and M. Di Renzo, "Beamforming Optimization for Active Intelligent Reflecting Surface-Aided SWIPT," in IEEE Transactions on Wireless Communications, 2022.

[57] Q. Qi, X. Chen, A. Khalili, C. Zhong, Z. Zhang and D. W. K. Ng, "Integrating Sensing, Computing, and Communication in 6G Wireless Networks: Design and Optimization," in IEEE Transactions on Communications, 2022.

[58] C. Wang, Z. Li, H. Zhang, D. W. K. Ng and N. Al-Dhahir, "Achieving Covertness and Security in Broadcast Channels with Finite Blocklength," in IEEE Transactions on Wireless Communications.

[59] D. W. K. Ng, E. S. Lo and R. Schober, "Robust Beamforming for Secure Communication in Systems With Wireless Information and Power Transfer," in IEEE Transactions on Wireless Communications, vol. 13, no. 8, pp. 4599-4615, Aug. 2014.